HHS Public Access

Author manuscript

Biotechnol Adv. Author manuscript; available in PMC 2022 October 13.

Published in final edited form as:

Biotechnol Adv. 2021 ; 49: 107753. doi:10.1016/j.biotechadv.2021.107753.

Building protein networks in synthetic systems from the bottom-up

Jiyoung Shim[a,1], **Chuqing Zhou**[a,1], **Ting Gong**[a,1], **Dasha Aleksandra Iserlis**[a], **Hamad Abdullah Linjawi**[a], **Matthew Wong**[a], **Tingrui Pan**[a,b,*], **Cheemeng Tan**[a,*]

[a]Department of Biomedical Engineering, University of California Davis, Davis, CA 95616, United States of America

[b]Suzhou Institute for Advanced Research, University of Science and Technology, Suzhou, China

Abstract

The recent development of synthetic biology has expanded the capability to design and construct protein networks outside of living cells from the bottom-up. The new capability has enabled us to assemble protein networks for the basic study of cellular pathways, expression of proteins outside cells, and building tissue materials. Furthermore, the integration of natural and synthetic protein networks has enabled new functions of synthetic or artificial cells. Here, we review the underlying technologies for assembling protein networks in liposomes, water-in-oil droplets, and biomaterials from the bottom-up. We cover the recent applications of protein networks in biological transduction pathways, energy self-supplying systems, cellular environmental sensors, and cell-free protein scaffolds. We also review new technologies for assembling protein networks, including multiprotein purification methods, high-throughput assay screen platforms, and controllable fusion of liposomes. Finally, we present existing challenges towards building protein networks that rival the complexity and dynamic response akin to natural systems. This review addresses the gap in our understanding of synthetic and natural protein networks. It presents a vision towards developing smart and resilient protein networks for various biomedical applications.

Keywords

Protein network; In vitro; Genetic circuit; Automation; High throughput; Bottom-up; Protein purification; Encapsulation; Artificial cell; Cell-free

1. Introduction

A typical cell contains approximately three million proteins per μm^3 (Milo, 2013). Despite the high number of densely packed proteins, they are arranged with the optimal level of spatial and temporal precision for the proper functioning of cells (Rafelski and Theriot, 2004). These proteins are also conceptualized as three-dimensional information processing

*Corresponding author at: Department of Biomedical Engineering, University of California Davis, Davis, CA 95616, United States of America tingrui@ustc.edu.cn (T. Pan), cmtan@ucdavis.edu (C. Tan).

[1]equal contribution

networks that process signals from the environment (Lenaerts et al., 2009). Here, we define a protein network as connected reactions involving at least two proteins. Thus far, our ability to construct protein networks outside cells pale in comparison to the natural cells.

A recent and concerted effort has been made to build artificial cells that contain complex protein networks from the bottom-up (Laohakunakorn et al., 2020; Wang et al., 2020). One purpose of building an artificial cell is to reproduce natural behavior with the minimum core-members of the cellular function of interest. Such reproduction allows us to study and define a single protein network without introducing the complexity of living cells. Along this line, cell receptor signaling cascades (Ding et al., 2018; Hui and Vale, 2014; Sangani et al., 2009), enzyme cascades (Hagan et al., 2010; Liu et al., 2019), membrane gate regulation (Hindley et al., 2019; Lentini et al., 2014), photosynthesis (Berhanu et al., 2019), and oxidative phosphorylation (Biner et al., 2016; Von Ballmoos et al., 2016) have been reconstructed in artificial cells from the bottom-up. These accomplishments are being leveraged to engineer biological transduction pathways (Su et al., 2016), energy self-supplying systems (Miller et al., 2020), and cell-free drug development systems (Cui et al., 2016).

A major hurdle to building protein networks from the bottom-up is our ability to efficiently purify multiple species of proteins. A common protein-purification method is the affinity chromatography approach. Although recombinant proteins without available tags are seemingly efficacious in the aspects of solubility and activity, a suitable protein-fusion tag enhances purification without a drastic effect on targeted protein properties (Gräslund et al., 2008). Through decades of development, many tag options are available for protein-tagging, such as glutathione S-transferase (GST, ~26 kDa), maltose-binding protein (MBP, ~42 kDa), and polyhistidine tags. Additionally, to ensure protein purity, the tandem affinity purification (TAP, ~21 kDa) tag requires two or more chromatography steps (Gloeckner et al., 2007). The N-terminal His-tag is also used for protein co-purification (Villarreal et al., 2018). The N-terminal His-tag is biochemically inactive and ensures bacterial transcription and translation (Gräslund et al., 2008). Furthermore, the N-terminal His-tagged protein can be immobilized onto artificial membranes containing lipids with a nickel-nitrilotriacetate head group. By employing this immobilization technique, protein networks have been reconstituted on liposomes (Hui and Vale, 2014) and supported membranes (Huang et al., 2016).

Building protein networks from the bottom-up also requires the development of automated and high throughput platforms. The representative technologies include contact-pin-printing (Jones et al., 2006; MacBeath and Schreiber, 2000; Swank et al., 2019), non-contact-inject-printing (Fan et al., 2017; Wang et al., 2019), and microfluidic-based continuous flow control (Weiss et al., 2018). A pin-printing system transfers DNA/protein to a substrate to screen thousands of reactions at the same time. Non-contact-nano/picoliter-inject-printing is controlled by various driving mechanisms for the high-throughput preparation of combinatorial assays. A microfluidic system can build protein networks inside liposomes or water-in-oil emulsion droplets. For example, chloroplast mimicking droplets are generated (Miller et al., 2020) in automated water-in-oil platforms. For measuring absolute affinities between molecules, an integrated microfluidic device is developed by mechanically induced

trapping of molecular interactions (MITOMI) (Maerkl and Quake, 2007; Swank et al., 2019).

We review the current examples and techniques for building protein networks from the bottom-up. Our examples cover protein networks that are reconstituted in lipid bilayers, water-in-oil droplets, and biomaterials. In addition, we summarize the modern technologies for compartmentalizing protein networks by inducing self-assembly or utilizing an automated assembly system (Fig.1). We envision this comprehensive review to inspire the widening and intensifying of bottom-up approaches to build protein networks in synthetic systems.

2. Protein networks in synthetic systems

2.1. Protein networks in droplets

Protein networks have been encapsulated in water-in-oil droplets. They have allowed for the recapitulation of actin cortices' dynamics, screening of protein-protein interaction, and identification of gene regulatory factors. A photosynthetic system was also created in vitro by coupling natural components to a synthetic enzymatic cycle.

While a lipid bilayer is chemically similar to the cell membrane, emulsion resembles the physical properties of the deformable cell boundary. Dynamic actin cortices were reconstituted in emulsions exhibiting spontaneous symmetry breaking (i.e., fractured or polar cortices) driven by myosin-induced cortical actin flows. The actin cortex is of particular interest due to its role in cell division, cell polarity, and motility. The actin cortex was formed at the inner interface of a droplet. Initially, ActA (Actin assembly-inducing protein) was localized at the interface and then led to the local activation of Arp2/3 (Actin Related Protein 2 and 3) and nucleation of a cortical actin network (Abu Shah and Keren, 2014). Briefly, recombinant protein ActA labeled Bodipy (green fluorescent dye) localized spontaneously to the water/oil interface due to its amphiphilicity and induced rhodamine-labeled actin polymerization (Abu Shah et al., 2015). The work revealed that mechanical forces were generated by the interplay between actin filament, structural proteins, and myosin motors. When *Xenopus* cell-free egg extracts were added, the physiological rate of actin disassembly was orders of magnitude faster than that without the extracts, accelerating cortical network dynamics. This cell-free reconstitution approach unveiled: i) the cortical dynamics are due to the interplay between myosin contraction and the connectivity of the networks, and ii) myosin is essential for cortical symmetry breaking. In addition, actin network architecture has been studied (Reymann et al., 2012) inside of giant unilamellar vesicles or at the supported lipid bilayers (Dürre et al., 2018; Köster et al., 2016).

Water-in-oil droplets are also directly amenable to high-throughput assays. One automated system generated approximately three million drops from a 25 μL reaction mixture, where Cui et al. (2016) created an in vitro protein affinity assay combining drop-based microfluidics with in vitro two-hybrid system (IVT2H). This mix-and-read drop-IVT2H was proven for screening the high-affinity peptide binders in a p53-MDM2 binding model. GFP (green fluorescent protein) was used as the surrogate reporter of gene expression. Gene expression from the promoter was modulated by the 'activation domain (AD)-MDM2',

'DNA binding domain (DB)-p53p (wild type p53 peptide) /PMI (synthetic duodecimal peptide)/PMI variants', and σ54-RNA polymerase holoenzyme (σ54-RNAP). The hybrid fusion proteins (AD-MSM2 and p53p/PMI-DB) and σ54-RNAP were expressed from three separated DNA constructs. The interaction between MDM2, p53p/PMI, and DB causes the binding of AD-MSM2 and p53p/PMI-DB near the promoter (Zhou et al., 2014). Initially, the DB was bound to the UAS (upstream activation sequence), and the AD, in close proximity to the promoter-bound σ54-RNAP, subsequently activated σ54-RNAP (Buck et al., 2000). The protein interactions then led to the GFP expression. After the off-chip incubation for the transcription and translation, the higher fluorescence intensity was observed in the droplets that encapsulated PMI-DB (K_d value for MDM2 -PMI (3.2 nM), –p53p (46 nM)). Fluorescence Activated Drop Sorting (FADS) device detected each droplet in a high-throughput and quantitative way to separate the droplet that had a fluorescence intensity above a threshold. These sorted droplets were analyzed and verified by DNA sequencing. This platform could be used to screen peptide-based drugs.

In addition, Fan et al. (2017) studied a multi-parametric genetic interaction by developing a microfluidic printing system with a disposable and multichannel cartridge design. The printing system could combine three different fluorescent proteins in various concentrations (i. e., 5 different concentrations of GFP * 4 mCherry * 3 TagBFP). It was scalable to multiple reagents, allowed the multiplexing of input reagents featuring at small volume, and minimized cross-contamination (see the details in Section 3.2). Using this printing system, they demonstrated the impacts of the reporter plasmid, a transcription factor (i.e., EsaR), and 3-oxo-hexanoyl-homoserine lactone (AHL) on transcription regulation of a cell-free system (Fig. 2A). In this system, the transcription factor EsaR binds to an operator site (i.e., EsaR box) that regulates the expression of a GFP reporter protein. AHL inducer binds to EsaR, relieving the repression of the promoter. They encapsulated plasmid Ngo1 (coding for GFP under control of a hybrid synthetic promoter T7/EsaR box), purified EsaR, and AHL with reaction buffer and protein mix. In each droplet, they allotted the same amount of the transcription-translation reaction mix but varied the concentration of the regulating factors. The results confirmed that the GFP expression level increased when plasmid and AHL concentration were increased, and EsaR concentration was decreased. The printing system allows for the study of genetic promoters and the identification of genetic regulatory factors.

In a recent work, Miller et al. (2020) reproduced chloroplasts within a water-in-oil droplet using the automated assembly of reaction compartments. This chloroplast mimicking droplet contained natural components of the thylakoid membrane and a synthetic enzyme cycle inspired by the Calvin–Benson–Bassham (CBB) cycle. It produced a multi-carbon compound (i.e., glycolate) through the light (50–60 μmol photons m^{-2} s^{-1}) -driven conversion of CO_2. Here, in the thylakoid membrane, photons of light were converted to electrons that were needed to produce NADPH (nicotinamide adenine dinucleotide phosphate) and ATP (adenosine triphosphate). These ATP and NADPH catalyzed the enzyme cascade consisting of the CETCH cycle (a catalytic cycle) that produced glyoxylate. Hahn et al. (2018) reconstituted chloroplasts ATP synthase by inserting intact cF_1F_O complex from spinach into lipid nanodiscs. Thus, photons of light essentially initiate the reaction, resulting in a light-driven reaction cascade. This artificial photosynthetic system

was optimized by adjusting the light intensities and varying internal molecular compositions. The microfluidic device was mounted on a microscope to observe NADPH fluorescence and light-activation of the thylakoid. A bar-coding technique was used to encode reaction conditions in the single droplet. In most cases, 4-bit emulsions were created and barcoded. This hybrid synthetic chloroplast had a carbon conversion efficiency of ~3.5% in droplets (NADPH consumption rate of CO_2 reduction/the measured maximum rate of $NADP^+$ photoreduction achieved in droplets). Overall, these technological advancements enable us to compartmentalize defined biological parts in a rapid, facile, and cost-efficient way.

2.2. Membrane-associated protein networks in liposomes

Protein networks can be established in vesicles surrounded by membranes. Vesicles bounded by phospholipid bilayer membranes, also known as liposomes, compartmentalize chemical reactions and control the substances going into and out of the liposomes. Membrane proteins can anchor to the liposomal bilayer membrane. In a protein network, they can function as signal transducers together with proteins encapsulated inside the liposomes or as membrane channels. Liposomes allow for the reconstitution of purified proteins and proteins expressed from inside the liposomes, which open novel approaches in protein research.

The liposomal membrane bilayer is a critical part of the bottom-up construction of protein networks because it creates a local environment with chemical properties similar to those of the lipid bilayer of biological cells. The fact that liposomes are artificially synthesized allows researchers to manipulate the composition of lipids in the liposomal membrane bilayer and the content of the cytosol. Sangani et al. demonstrated that a supporting lipid membrane (composed of phosphatidylserine) allowed for the reconstitution of PiYLAT, a tyrosine-phosphorylated recombinant variant of the transmembrane adaptor protein linker for activation of T cells. They also demonstrated the formation of a cooperative protein network (see the method in Section 3.3.5) with high-avidity protein signaling complexes (Sangani et al., 2009).

Liposomes also allow for a faster reaction rate of anchored proteins than proteins in solution. For instance, Hui and Vale found phosphorylation rates for both pre-liposome-anchored Lck and CD3ζ to be several hundred-fold faster than in solution at their physiological densities and a positive correlation between the phosphorylation rate and the protein densities. They reconstituted the T-cell receptor (TCR) proximal signaling network by adding purified enzymes to liposomes to recreate a suitable chemical environment in the membrane bilayers for these enzymes to interact (Hui and Vale, 2014). By varying enzyme concentrations (i.e., pre-binding Lck, CD45, and CD3ζ to liposomes), combining them in various ways, and performing kinetic and steady-state readouts of de/phosphorylation, this simplified system provided relevant information for understanding the functions of these enzymes (see the method in Section 3.3.5).

In addition, the anchoring of proteins to liposomes allows for the localized crowding of the proteins. A study by Zhang et al. (2006) used liposomes to study the activation of the epidermal growth factor receptor (EGFR) network. The use of liposomes allowed for the localization of the EGFR kinase domain to the surface of the vesicles, which subsequently allowed for a controlled increase in the local concentration of kinase. The EGFR kinase

domain was found to be able to be activated by an increase in its local concentration or a mutation in its L834R leucine residue in the activation loop. They formed small unilamellar vesicles of around 100–200 nm from 1,2-dioleoyl-sn-glycero-3-phosphocholine (DOPC) and 1,2-dioleoyl-sn-glycero-3-{[N-(5-amino-1-carboxypentyl) iminodiacetic acid] succinyl} nickel salt (DOGS-NTA-Ni) lipids with a nickel-nitrilotriacetate head group to localize the hexahistidine tagged EGFR kinase domain to it. It allowed researchers to vary the mole ratio of DOGS-NTA-Ni to DOPC in the membrane to test how the concentration of nickel-nitrilotriacetate head groups regulated the activities of different domains (Zhang et al., 2006).

Another study by Monsey et al. (2010) found that the kinase-specific activities of Her4 and Her2/neu (other domains of the EGFR family) increased 40-fold and 3.5-fold respectively, when they bound to nickel-liposomes. In these studies, liposomes created a well-defined in vitro reaction environment that resembled the physiological conditions of biological cells. The liposome membranes also resembled the membranes of biological cells, which provided a native environment for natural proteins. The alteration of membrane composition, the addition of different concentrations, and the combination of purified enzymes created novel approaches to study protein interactions (Hui and Vale, 2014).

Based on the understanding of lipid membranes, membrane proteins can be incorporated into the liposomal membrane bilayer to interact with proteins inside the liposome. This protein-membrane-membrane protein interaction (P1-M-P2) is the basis of protein signaling pathways in liposomes. Hindley et al. (2019) established a sPLA2(P1)-MMscL(P2) network in liposomes where the mechanosensitive channel of large conductance (MscL), a homopentameric integral membrane protein, responded to signals from secretory phospholipase A2 (sPLA2). The membrane proteins then opened a pore in the membrane to release substances inside the cell. This network could be activated by increasing calcium concentration inside the liposomes. It could also be coupled to a functional output. The signal could then be amplified by using a membrane opener, αHL (α-hemolysin), to let calcium (a key messenger) permeate the liposomes. The ability of protein networks to be activated or amplified in liposomes forms the foundation for practical applications such as drug delivery and biosensing.

Furthermore, liposomes can be functionalized using multiple membrane proteins. By using the SNARE protein-based method (see details in Section 3.3.4), Nordlund et al. (2014) incorporated three multisubunit membrane proteins, bo3 oxidase, fumarate reductase, and ATP synthase, into the liposomal membrane to deliver large water-soluble substrates into the liposome. The liposomes were constructed by first reconstituting bo3 oxidase and ATP synthase into a liposome sample, then reconstituting fumarate reductase into another, and subsequently mixing the two samples afterward, allowing the liposomes to fuse. Ultimately, they reconstructed a fully functional respiratory chain in the liposome. Similar studies were done by Biner et al. to reconstitute bo3 oxidase and ATP synthase into unilamellar liposomes (Biner et al., 2016). By allowing the incorporation of multiple membrane proteins, complex protein networks can be reconstituted in liposomes. The reconstitution of protein networks in liposomes opens the possibility of using liposomes as a tool to study natural protein interactions and as artificial cells for therapeutic applications.

Protein networks in liposomes can also interact with protein networks in other liposomes and bacterial cells. Ding et al. (2018) constructed a sender circuit and a receiver circuit in liposomes. The sender circuit consisted of EsaI that catalyzed the synthesis of an acyl-homoserine lactone (AHL). The receiver circuit consisted of a PT7-EsaR promoter that expressed a green fluorescent protein (GFP). The promoter was inhibited by the binding of EsaR, which in turn could be released by the binding of AHL (Ding et al., 2018). In another study, liposomes containing isopropyl β-d-1-thiogalactopyranoside (IPTG) were engineered to synthesize pore-forming protein α-hemolysin (αHL) in the presence of theophylline, which triggered the release of IPTG. IPTG then induced the synthesis of a fluorescent protein in *E. coli* (Lentini et al., 2014). These studies demonstrated that liposomes could be engineered to communicate with bacterial cells using protein networks (Rampioni et al., 2018). Apart from *E. coli*, liposomes can also send signals to other bacterial cells, including *Vibrio fischeri*, *Vibrio harveyi*, and *Pseudomonas aeruginosa* (Lentini et al., 2017). In addition, Adamala et al. (2017) engineered genetic circuits and cascades allowing for communication between different populations of liposomes. For instance, a sensor liposome expressed αHL upon induction by arabinose. The αHL then created pores that release IPTG from the sensor liposomes. After which, the released IPTG induced fLuc (firefly luciferase) expression in the reporter liposomes. These results show that protein networks in liposomes can send signals to and interact with both liposomes and living cells, making them viable options for drug delivery and therapeutic applications.

Liposomes serve another unique function by allowing denatured membrane proteins to be reconstituted in their native, functional structures. Hagan et al. showed that the chaperone SurA delivered denatured outer membrane protein (OmpT) to the beta-barrel assembly machine (Bam) complex, which refolded the denatured OmpT into a functional configuration (Hagan et al., 2010). Another study showed that purified peripheral myelin protein 22 (PMP22) could be reconstituted in lipid vesicles that resembled the organization of compact myelin of peripheral nerves in vivo (Mittendorf et al., 2017). The ability of liposomes to reconstitute denatured proteins demonstrates the potential for liposomes to be used as a tool to study the formation and interactions of membrane proteins.

2.3. Minimal genome and energy-producing protein networks in artificial cells

Liposomes also allow for the reconstitution of protein-synthesis systems that can express proteins from the inside of giant vesicles (Fujii et al., 2013; Garamella et al., 2019; Stano, 2019; Tan et al., 2013). The pioneering research has enabled the study of information propagation in protein networks and the development of synthetic protein networks with novel functions.

A number of proteins, including Sec translocon (Matsubayashi et al., 2014), cytochrome *b*(5) (b5) (Nomura et al., 2008), α-hemolysin pore protein from *Staphylococcus aureus* (Noireaux and Libchaber, 2004), and Connexin-43 (Cx43) (Moritani et al., 2010) were synthesized from their genes and reconstituted in liposomes. The bottom-up reconstruction of protein networks in liposomes facilitated the study of the structures and functions of mutant proteins (Matsubayashi et al., 2014) and the conditions needed for membrane proteins to integrate and function properly as there were fewer unknown components in

the liposomes that might interfere with the analysis (Moritani et al., 2010). Recently, Godino et al. (2019) expressed Min proteins from their genes in liposomes, where the synthesized proteins could oscillate between the membrane and the lumen of the liposomes. The recruitment of the Min proteins to the inner surface of the liposomal lipid bilayer resulted in the dramatic deformation of the shape of the liposomes. One of the Min proteins, MinC, is an inhibitor of the FtsZ polymerization, which in turn is a sign of the onset of cell division. Here, Godino et al. showed the potential for the construction of functional synthetic cells from a minimal genome. The minimal genome represents a reduced set of genes that are necessary for the proper functioning of a synthetic cell. The work (Godino et al., 2019) allowed for the observation of Min oscillating patterns and membrane deformation in real-time.

One application of reconstituting protein networks from genes is the production of energy independent artificial cells. Berhanu et al. (2019) expressed an ATP synthase F_OF_1 and bacteriorhodopsin (bR) in proteoliposomes, which conferred the ability to produce ATP from light. They were combined with a PURE system that synthesized F_OF_1 and bR. The protein networks were encapsulated in giant unilamellar vesicles (GUVs). The synthesized F_OF_1 and bR, in turn, produced more ATP under illumination, essentially creating a positive feedback loop. This photosynthetic cell was one of the first energetically independent artificial cells produced. The energy-producing pathway could potentially be coupled with other synthetic pathways. Here, protein networks are demonstrated to produce self-sufficient artificial cells that can be used to synthesize high quantities of drugs and biomaterials continuously with minimal energy input (Fig. 2B). Lee et al. (2018) generated giant vesicles that produced ATP from light. An ATP synthase and two photo-converters, plant-derived photosystem II and bacteria-derived proteorhodopsin, were reconstituted into the membrane of liposomes. These liposomes were then encapsulated in a giant vesicle. Independent optical activation was achieved where ATP synthesis was activated by red light but impeded by green light. When coupled with carbon fixation and actin polymerization reactions, both of which were ATP-dependent, this system successfully achieved optical control of both reactions.

Overall, the technology of synthesizing proteins through cell-free systems in lipid vesicles has been well-established in recent years. These studies have great impact on deepening our understanding of protein networks. They also open the door to creating artificial cells that can perform novel functions beyond the possibility of natural evolution.

2.4. Signaling protein networks in planar materials

While liposomes could provide a shell-like bilayer lipid membrane to avoid the direct exposure of the encapsulated proteins to the outside environment, it becomes challenging to monitor surface events on the bilayer lipids (Bally et al., 2010). Protein networks in synthetic systems have been used in conjunction with planar biomaterials to enable the characterization of complex signaling pathways, the development of novel protein scaffolds, and novel applications in tissue engineering. Current synthetic biology approaches allow for extensive control and modulation over the interaction between the protein networks and the desired biomaterial.

Recent use of protein networks focuses on protein clustering. This phenomenon has been observed in numerous cell receptor signaling cascades. Despite the prevalence of this phenomenon in many biologically relevant signaling cascades, the mechanism of cluster formation and the influences of protein clustering on signal propagation remains unclear. This issue is partly due to the difficulty in isolating the role of specific proteins in the formation of the cluster, and specifically elucidating the impact of cluster formation on signal enhancement. However, the bottom-up reconstitution of cell signaling cascades onto planar biomaterials, such as supported membranes, provides an ideal platform for the detailed investigation and unraveling of how these complex clusters form and their influence on signaling. T cell receptor signaling (TCR) is one such signaling pathway that implements protein cluster formation (Su et al., 2016). Specifically, in TCR signaling, it is known that the transmembrane protein LAT (linker for activation of T cells) is crucially involved in the initiation and formation of the protein cluster, as was proven in studies of cell lines that lacked the LAT protein. However, the mechanism by which LAT promotes cluster formation, what other proteins are crucial to cluster formation, and how clustering affects the kinetic of these proteins were not well understood. By reconstituting LAT in synthetic systems, the specificities of cluster formation were extrapolated.

To reconstitute this key section of the TCR signaling pathway, purified LAT was integrated into supported bilayers (Su et al., 2016). LAT was fixed to the membrane by the addition of His8 tag to the N-terminus of LAT, while the lipid bilayer was coated with Ni^{2+}. After LAT fixation, key sections of the signaling pathway could be formed by their addition in solution. This stepwise approach of reconstituting the pathway enabled the identification of other key proteins in LAT clustering, what biochemical reactions promoted cluster formation, and the behavior of the cluster when formed. Specifically, the binding of an adapter protein, either Grb2 or Gads, and the consequential association with either Sos1 or SLP-76 were found to be the two crucial conditions for cluster initiation. Additionally, the presence of phosphorylated tyrosines on LAT was essential to cluster formation. They served as the site of Grb2 or Gad conjugation, with clusters breaking up upon dephosphorylation of LAT and not reforming until LAT was re-phosphorylated. Furthermore, the reconstituted protein network allowed for the characterization of cluster behavior. Fluorescence recovery revealed that these clusters became phase-separated from the membrane and behaved as dynamic fluids, with various proteins entering and leaving the fluid-like cluster. Finally, the bottom-up system revealed the downstream signaling effects of clustering. Two phosphorylated tyrosines were found to be the minimum number for the cluster formation of LAT. Downstream initiation of Arp2/3 (actin-related protein 2 and 3) could begin actin bundle formation, a typical response of T cells after receptor initiation.

Cell-free protein networks can also be used to study the kinetics of reactions that interact with planar biomaterials (Huang et al., 2016). For instance, Huang et al. investigated how protein clustering (also called protein assembly) alters the kinetics of T cell receptor protein. The synthetic system was similar to the one used by Su et al. (2016), where they assembled T cell receptor cascades onto lipid bilayers by exploiting the His-tag Ni^{2+} association (Huang et al., 2016). In order to quantify the kinetic influence of protein clustering, single-molecule dwell time was used to measure the assembly time of the LAT:Grb2:SOS cluster. The results indicated that cluster formation aided in the formation of two kinetically distinct

response mechanisms in the signaling cascade. These differing mechanisms ensured that signal propagation was noise-resistant and occurred only when the T cell receptor was properly activated.

In both studies, the reconstitution of complex protein networks allows for the understanding of previously poorly understood protein networks. By taking a stepwise approach to the reconstitution of these protein networks, the specific interactions and proteins underlying the phenomenon can be elucidated. Furthermore, robust experiments validating these interactions can be performed. This achievement opens the door for using protein networks to isolate and study other previously poorly understood complex protein networks that interact with various biomaterials.

2.5. Protein networks in scaffolds

In addition to characterizing protein networks and their interactions with planar biomaterials, protein networks have also been utilized to develop novel protein scaffolds, which function as the biomaterials upon which multi-enzyme assemblies can be formed. Protein scaffolds can alter and enhance the kinetics of multi-enzyme pathways by applying spatial control over enzymatic reactions and minimizing the diffusion time of reaction intermediates. Thus, an encodable, self-assembling protein scaffold whose docking domains can be easily altered was a desired product in the field. The ability of modular protein scaffolds was first revealed in Dueber et al. seminal work (Dueber et al., 2009). They implemented various interaction domains to create a linear substrate channeling protein scaffold. When the designed scaffold was paired with a mevalonate production pathway, the pathway's production of mevalonate was increased 77-fold, to a titer of 5 mM. This work has inspired the design and implementation of linear substrate channeling protein scaffolds to other biosynthetic pathways (Moon et al., 2010).

To increase spatial control over biosynthetic pathways, Liu et al. developed modular non-linear protein scaffolds (Liu et al., 2019). The protein scaffold was formed with an elastin-like polypeptide (ELP) backbone that had site-specific reactive peptide tags at the ends. These tags were either the SpyCatcher or SpyTag. Depending on which combination was on the backbone, a different protein scaffold would form. An ELP backbone with either two SpyTags or two SpyCatchers would form a crosslinked scaffold composed of multiple linked single scaffold proteins, while an ELP backbone with both a SpyTag and SpyCatcher would cause the protein to bind to itself, forming a cyclic scaffold. To prove the functionality of these scaffolds, both scaffold types were expressed with specific docking domains embedded into the ELP backbone. Furthermore, enzymes from the menaquinone biosynthetic pathway, MenD, and MenH, were expressed with docking domains that complemented the ones expressed in the scaffolds. The cell-free nature of the system allowed the effects of the biomaterial protein scaffold on the menaquinone multi-enzyme assembly to be studied. The catalytic capacity and kinetics of MenF, MenD, and MenH were compared between the free enzyme state, assembled onto the crosslinked protein scaffold state, and assembled onto the cyclic protein scaffold state. Within 12 min, the crosslinked assembly had a catalytic yield of 94.4%, the cyclic assembly had an efficiency of 93.7%, and the free enzyme reaction had a catalytic yield of only 76%. Moreover, a kinetic analysis of the reaction revealed that while

both scaffolds increased the catalytic yield of the reaction, they did so through different kinetic mechanisms as a result of the different ways in which the multi-enzyme network formed around the protein scaffold (Fig. 2C).

Overall, the results highlight the potential for engineered protein scaffolds to increase the catalytic efficiency of various multi-enzyme reactions. These results also reveal how different scaffold structures influence the kinetics of multi-enzyme assemblies. Moreover, these results illustrate yet another avenue where protein networks have expanded potential applications. As demand for products of biosynthetic pathways increases, the ability of protein networks to develop, test, and modulate catalytically active protein scaffolds can be crucial to meeting the demand for these products.

2.6. Protein networks in engineered tissues

Leveraging the ability to build protein networks in liposomes and planar materials, protein networks can be used to functionalize extracellular matrix (ECM) of engineered tissues. The ECM plays a critical role in the differentiation efficiency of stem cells, cell signaling, and cell proliferation. Synthetic ECM often lacks the complexity of native ECM, while native ECM often poses an immunogenicity risk. However, cell-free manufacturing of ECM protein networks has emerged as a promising solution to the need for reliable, non-immunogenic, and reproducible ECM.

Synthetic ECM was constructed by exposing the protein-protein binding domains in ECM proteins like fibronectin, laminin, and collagen type I and IV, whose binding domains are typically hidden within the fully folded globular proteins (Feinberg and Parker, 2010). This change in protein conformation was triggered by depositing the folded proteins into hydrophobic mediums and then transferring them to a hydrophilic surface, where the now exposed binding domains caused ECM nanofiber formation. Specifically, a contact micro printer with a hydrophobic polydimethylsiloxane stamp was used to print linear strands of ECM proteins, either single protein prints or combinations of ECM proteins, into anhydrous poly(N-isopropylacrylamide). Once transferred, the now denatured proteins with their binding regions exposed, began to assemble into ECM nanofibrils. Finally, the anhydrous poly(N-isopropylacrylamide) medium was melted away, leaving only the fully formed protein nanofabrics. To test their viability as functional ECM, cardiomyocytes were cultured on these nanofabrics. The cardiomyocytes were able to be cultured on the nanofabrics, with no adverse cytotoxicity. Additionally, the nanofabrics were able to support the formation of mechanical and electrical cardiac contractions and cycles.

Using similar principles of surface-initiated assembly, Palchesko et al. reconstituted corneal basement membranes (Palchesko et al., 2016). As was done in Feinberg's study (Feinberg and Parker, 2010), the ECM proteins, collagen type IV, and laminin, first had their binding domains exposed in a hydrophobic medium. The proteins were then transferred via microcontact printing to a less hydrophobic medium where assembly could initiate (Palchesko et al., 2016). Finally, these assembled ECM proteins were transferred to collagen-type-I gel. Multi-photon imaging and atomic force microscopy (AFM) verified that this protein network had assembled and formed a dense basement membrane. Moreover, the viability of the developed basement membrane was validated, when bovine corneal epithelial

cells maintained a viable monoculture that continued to express phenotype markers. The findings in the two referenced studies shed light on the possibility of cell-free printing and the formation of tissue-specific ECM. The findings also open the door for other applications that can take advantage of protein-biomaterial interactions to form useful protein networks and materials.

Taken together, the findings illustrated in this section highlight the ability of a protein to interact with planar biomaterials and shed light on complex protein biomaterial interaction. These efforts can lead to new protein-based biomaterials with industrially significant effects. Furthermore, synthetic ECM can be engineered to recapture the complexity of native ECM. However, these applications share a common challenge in that they are often constrained by the ability to produce and purify the necessary proteins. Despite this constraint, the combination of proteins and biomaterials constitutes a modular system that can be optimized for novel applications and studies.

3. Bottom-up assembly methods of protein networks

3.1. Multiprotein purification

To build protein networks from the bottom-up, high-throughput methods to synthesize the protein components are critical. Tremendous protein purification methods have been successfully developed in the last 20 years. The purification methods use a broad range of purification peptide tags, including peptide hexahistidine (His) (Hochuli et al., 1987), calmodulin-binding peptide (CBP) (Stofko-Hahn et al., 1992), covalent yet dissociable (CYD) (Kimple and Sondek, 2002), Strep II (Voss and Skerra, 1997), FLAG (Brizzard et al., 1994), heavy chain of protein C (HPC) tags (Stearns et al., 1988), and the glutathione S-transferase (GST) (Smith and Johnson, 1988) and maltose-binding protein (MBP) (di Guana et al., 1988). The fusion tags result in different purity, yield, and cost of protein purification. For instance, His tag allows for moderate purification yield from *E. coli* extracts, but relatively poor purification yield from BY4742 yeast, Oregon R *Drosophila*, and HeLa-S9 extracts (Lichty et al., 2005). CBP tag produces moderate purity of protein from BY4742 yeast, *E. coli*, and Oregon R *Drosophila* extracts, but relatively higher purity from HeLa-S9 extracts (Lichty et al., 2005). Epitope-based tags, such as FLAG and HPC, produce the highest purity of protein for various cell sources (Lichty et al., 2005). GST tag can increase the solubility of proteins from prokaryotes (Kimple et al., 2013). Integral membrane protein has been labeled with modified His-tag, truncated and mutated version of GST, streptavidin-tag, SUMO (small ubiquitin-related modifier) tag, and MBP for purification (Hu et al., 2008; Ma et al., 2015; Quick and Wright, 2002; Rahman et al., 2007; Zuo et al., 2005). The purification techniques of peripheral membrane proteins are milder than integral membrane proteins, and are similar to the approaches used for cytoplasmic proteins.

The typical procedure for purifying proteins involves ion exchange (IEX) or mixed-mode chromatography to separate target protein fraction from cell culture or serum (Gloeckner et al., 2007). Further chromatographic steps are applied to achieve the desired purity level. To collect multiple types of pure proteins at once, mixed-mode chromatography resin with various ligands (IEX, affinity, and mixed-mode) can be used to obtain purified fractionation of small-volume protein samples. AcroP-repTM Advance 96-well filter plates combined

with Pall chromatography media can separate three proteins in a protein sample. This utilization of a filter plate-based strategy makes rapid screening of multiple purification schemes possible and helps optimize larger-scale purification. Similarly, combining a tandem Strep-tag II with a FLAG-tag allows for the elution of SF-tagged proteins under native conditions, which allows for fast purification of protein complexes from mammalian cells within 2.5 h (Gloeckner et al., 2007).

Another way to increase the efficiency of purifying multiple proteins is through the usage of automated protocols. Automated protocols were designed to purify proteins with minimal operator intervention (Camper and Viola, 2009). First, the efficiency of several key steps, including automated sample loading, column washing, and sample elution, were tested. The efficiency of peak collection steps for ion-exchange, metal affinity, hydrophobic interaction, and gel filtration chromatography were also evaluated. Permutations of these individual methods were tested individually and sequentially to achieve fully automated and optimized purification of a target protein. In another application, automated multistep purification of $(His)_6$- and Glutathione S-transferase (GST)-tagged proteins was achieved by using ÄKTAT 3D system (Sigrell et al., 2003). This system minimizes the preparation, run-time, and repetitive manual tasks, making it possible to purify up to 6 different His_6- or GST-tagged proteins per day and can produce 1–50 mg protein per run at >90% purity. In a recent study, by applying NGC chromatography system (Bio-Rad), up to five samples were automatically purified using a three-step purification procedure (Becker et al., 2019) (Fig. 3A). Through designing the first chromatographic step followed by a desalting step and setting size exclusion chromatography as a final purification step, this configuration could purify 150–200 mg protein at high quality and purity.

To assemble a protein network without multiple cultures, 34 key proteins containing 3 initiation factors, 4 elongation factors, 3 termination/release factors and the ribosome recycling factor and 23 AAT (aminoacyl-tRNA transferases) were co-expressed in 15 or 34 *E. coli*-strains consortia (Villarreal et al., 2018). 34 different kinds of proteins were successfully purified by using an efficient His-tag purification method. Without further manipulation, the 34 proteins constituted minimal cell-free translation machinery that could synthesize proteins. Based on the above research, a new cell-free system was recently achieved (Contreras-Llano et al., 2020) (Fig. 3B). This new cell-free system used a holistic approach, in which local modules were expressing translation machinery that changed the expression levels of more than 700 proteins. The proteome re-programming led to 5-fold higher expression level of different types of proteins (fluorescent reporters, protein nanocages, and the gene-editing nuclease Cas9). Another work from Jewett et al. (2013) developed a one-step co-activation method for integrated rRNA synthesis, ribosome assembly, and translation (iSAT), where mRNA could be translated by newly assembled ribosomes. Based on iSAT, Hammerling et al. (2020) selected active ribosomal genotypes from a ~ 1.7×10^7 member library of ribosomal RNA variants and identified their antibiotic resistance.

3.2. Microfluidic and robotic platforms to assemble protein networks

After purifying the protein components, the next step is to assemble the networks from the bottom-up. Due to the advantages of the cell-free format, different network variants can be assembled at high-throughput by mixing proteins with different mechanisms of action at multiple concentrations. Nowadays, robotic liquid handling platforms have been widely used to automate traditional manual pipettes. The robotic platforms can minimize human errors and improve operational efficiency (e. g., Fluent™ from Tecan) in the large-scale screening assay. However, these automated pipettes-based platforms are suitable for preparing assays in the size of tens or hundreds of microliters. This size constraint limits their uses in quantitative reconstitutions of protein networks, due to the high cost of purified proteins. To overcome the challenge, various technologies for handling small volumes of liquid have been established, including contact pin printing, non-contact inject printing, and microfluidic-handling of water-in-oil droplets.

Pin printing uses a manifold of pins to transfer small aliquots of a sample library to a receiving substrate, featuring a simple operation process and ultrahigh scalability (e.g., Qarray2 from Genetix, GMS 417 Arrayer from Affymetrix) (MacBeath and Schreiber, 2000; Swank et al., 2019) (Fig. 4A). The transferred liquid volume is determined by a variety of conditions, including the materials and geometry of the pins, the wetting characteristics of the substrate, and the moving speed (Müller and Papen, 2005). In most cases, precise volume control over the pin printing demands micro-machined pins and micro-fabricated substrates. 159 protein binding domains and 66 ErbB tyrosine residues were quantitively studied on a protein array with eight concentrations of each peptide ranging from 10 nM to 5 μM. It enables the study of the ability of each receptor to respond upon activation of a signaling pathway (Jones et al., 2006). However, due to the intrinsic contact between the pin and the substrate, it causes cross contaminations while transferring multiple reagents on the same spot (Lalo et al., 2009). The issue limits its applications in multiplexing protein assays.

Non-contact nanoliter/picoliter inject printing has also been used due to its high precision in controlling droplet size and efficiency in creating combinatorial arrays. Contrary to contact pin printing, droplets can be generated in a small orifice that can be precisely controlled by driving forces, including electromagnetically actuated pins (Ding et al., 2013), piezoelectric actuators (Fan et al., 2018; Li et al., 2015), and pneumatic drives (Li et al., 2018) (Fig. 4B). Currently, most low-volume injecting systems employ piezoelectric actuators to apply a mechanical stroke on the continuous liquid flow, which can form droplets via the process pinch-off. However, these commercial dispensers are not disposable due to the high manufacturing cost that arises from the complex mechanical designs of the dispensers. Then, cumbersome washing and reagent-waste priming processes are required to minimize the cross-contamination among reagents, which limits its applications in screening protein networks.

Addressing the issue above, Fan et al. (2017) developed a microfluidic multi-parametric impact printing system that was adapted to a plug-and-play disposable, multichannel microfluidic cartridge. The cartridge was assembled by integrating a reservoir layer, an elastic membrane layer, a microchannel layer, and a bottom nozzle layer, where the liquid was physically separated from the actuators. The droplet was generated by striking the

deformable membrane near the nozzle to squeeze the liquid out, enabling the generation of droplets in the range of 100 pL-10 nL, which led to 1–10,000-fold dilution in a 1 μL. This system has been successfully used in the modeling of molecular interactions of GFP-plasmids, EsaR, and AHL over a wide range of concentrations. Compared with high-cost industrial dispensers, disposable microfluidic cartridges are more suitable for biological assays. Still, the scalability of the system is limited by the high cost of scaling up and calibrating the increasing number of actuators. Wang et al. (2019) further established a pipette-free robotic-dispensing system, which used a microfluidic-enabled container cap to achieve seamless integration of liquid handling and robotic operations. By sharing the actuator on a robotic arm, this system performed large-scale multi-reagent dispensing tasks without limiting the number of reagents. To better study protein networks, the surface treatment of the microfluidic cartridge might be necessary to minimize the absorption and clogging of proteins before printing.

Acoustic injection technology has been established to transfer liquid from one container to a substrate by a focused acoustic device, without the uses of pipettes tips, pin tools, or ejection nozzle (Fig. 4C). The droplet volume can be varied from 1 pL to 1 μL by changing the ultrasound frequency in the range from 1 to 200 MHz (Hadimioglu et al., 2016). Due to the sensitivity of the acoustic energy to liquid acoustic property, fluid height, and the material of the container, it is necessary to detect the fluid in each container and calibrate the droplet size before ejecting droplets. Currently, a commercial acoustic liquid handling system can transfer as many as 500 samples per minute from 384-, 1536-, and 3456-well plates to any substrate (e.g., Echo™ from Labcyte). Using this acoustic printing technology, Moore et. Al. have established a quantitative model of a gene regulatory network in a nonmodel bacteria, *Bacillus megaterium*, where purified XylR promoter was characterized with different concentrations of XylR repressor proteins, D-xylose, and DNA template (Moore et al., 2018). This study shows that the acoustic liquid handling robots may be used to assemble a broad range of protein networks.

In addition to processing low reaction volume, microfluidic technology can be used in detecting transient and subtle protein events. A microfluidic device, the mechanically induced trapping of molecular interactions (MITOMI), was fabricated by multilayer soft lithography and bonded to a DNA microarray. It contains 2400 reaction spots controlled by 7233 on-chip Quake valves, where the deflectable button membrane could be brought into contact with a protein-bound surface, which minimizes the loss of proteins during the washing. It has been applied to screen DNA binding energy landscapes for four eukaryotic transcription factors covering titrations over 464 target DNA sequences (Maerkl and Quake, 2007). The MITOMI device has been designed to generate the variants of repressors and promoters of the zinc-finger family transcription factors by using on-chip PCR assembly. It allows 768 cell-free reactions to be performed using 124 promoter variants that cover all possible single-base mutations within the −47 to −7 region of the λP_R promoter (Swank et al., 2019).

Another type of vesicle-handling microfluidic devices, such as the T-junction and cross-junction, became widely employed to produce lipid-based large or giant unilamellar vesicles (LUVs or GUVs). These vesicles can be used for the study of metabolic signaling

or synthesizing activities under controlled environments. When compared to traditional methods of forming water-oil-water vesicles, droplet-based microfluidics can process very limited samples with high precision and high throughput (Shembekar et al., 2016) (Fig. 4D). Recently, researchers have added sub-cellular compartments into LUVs or GUVs to form complex artificial cellular systems. Abate et al. demonstrated that the applied electrical field could destabilize the distribution of charges at the intersurface, allowing an injected droplet in the range of 0.1 pL to 3 pL to fuse into a preformed vesicle (Abate et al., 2010). Recently, Weiss et al. successfully added sub-cellular compartments into LUVs or GUVs to form complex artificial cellular systems, where purified transmembrane and cyto-skeleton proteins were injected into GUVs by the electro coalescence-based microfluidic injection technology (Weiss et al., 2018). Although this technology is not ready for the large-scale screening of protein networks, it permits the manipulation of the contents of LUVs or GUVs.

3.3. Self-assembly of protein networks

In contrast to microfluidic devices that require external intervention, self-assembly methods exploit physical interactions between membranes to assemble protein networks. Self-assembly of membrane proteins has been achieved by the photoinitiated polymerization, by rehydrating GUV over agarose layer, by charge-mediated fusion, or by protein-mediated fusion. Another common method is to immobilize purified and tagged membrane proteins on a lipid membrane with the corresponding affinity tags. These methods help to enable broad ways to assemble protein networks in synthetic systems.

3.3.1. Photo-PISA—Conventional self-assembly methods have difficulties when inserting hydrophobic biomolecules, such as membrane proteins into vesicles (Varlas et al., 2018). Photo-PISA (photoinitiated polymerization-induced self-assembly) makes it possible to synthesize membrane protein-vesicle complexes, even with hydrophobic biomolecules. Photo-PISA has been used to incorporate an insoluble outer membrane protein (OmpF) into polymeric self-assemblies in the presence of surfactants. The prior work explored the physical interaction and effect of different types of small-molecule surfactants (i.e., critical micelle concentration (CMC) values and nature) on the process of self-assembly of a poly (ethylene glycol)-b-poly (2-hydroxypropyl methacrylate) (PEG-b-PHPMA) block copolymer system (Varlas et al., 2018). Photo-PISA works by first creating a water-soluble poly(ethylene glycol) macro-chain-transfer-agent (PEG_{113}-CEPA mCTA) by esterifying an acid functionalized chain-transfer agent (CEPA CTA) with a poly(ethylene glycol) monomethyl ether homopolymer (PEG_{113}-OH). PEG_{113}-CEPA mCTA subsequently undergoes chain-extension when mixed with a water-miscible monomer, 2-hydroxypropyl methacrylate (HPMA). This PEG_{113}-CEPA mCTA and HPMA mixture is then supplemented with horseradish peroxidase (HRP) and OmpF that has been stabilized in an aqueous surfactant solution. This mixture results in a polymerized solution that, when irradiated at 405 nm, full monomer conversion occurs, and the protein is fully reconstituted (Varlas et al., 2018). In consequence, the stabilized OmpF was reconstituted into the PHPMA membrane of PEG_{113}-b-$PHPMA_{400}$ vesicles by a one-pot photo-PISA reaction. OmpF was purified and stabilized in a solution composed of non-ionic surfactants, DDM, and sodium phosphate. This procedure did not affect the protein's secondary structure or

vesicular morphology. HRP was used for the read-out of OmpF function (permeability) by colori-metric assays employing o-dianisidine. The vesicle's size and membrane thickness can be tuned by changing the type of surfactant and its concentration. It has been demonstrated that non-ionic surfactants, as well as zwitterions at low concentrations, retain vesicular morphology even under changing concentrations. Conversely, ionic surfactants or an increase in zwitterionic surfactant concentration cause vesicles to adopt large interfacial curves or undergo morphological changes, respectively (Varlas et al., 2018). Hence, it is imperative to select a non-ionic surfactant or zwitterionic surfactant at a low concentration to retain a properly shaped vesicle for the incorporation of a hydrophobic molecule. Through aqueous photo-PISA, mixed block copolymer/surfactant vesicles have been created.

3.3.2. Agarose rehydration—While Photo-PISA allows for the incorporation of membrane proteins into membranes, it is still challenging to encapsulate proteins in ionic solutions into liposomes. Electroformation and gentle hydration are primarily used to determine phase separation in model membranes, but these methods are incompatible with proteins as they are too protein disruptive (Gutierrez and Malmstadt, 2014). Agarose rehydration, a less destructive method, rehydrates GUVs over thin layers of agarose composed of dissolved proteins to incorporate the proteins into the GUVs (Gutierrez and Malmstadt, 2014).

For instance, recent work incorporated G protein-coupled receptor 5-HT_{1A} (5-hydroxytryptamine receptor subtype 1A) into GUVs and observed the receptor in phase-separated vesicles (Gutierrez and Malmstadt, 2014). The GUVs were made from a ternary mixture that underwent phase separation at certain temperatures and compositions. It consisted of 1-palmitoyl-2-oleoyl-*sn*-glycero-3- phosphocholine (POPC), cholesterol (Chol), and brain sphingomyelin (BSM). A fluorescent lipid, ATTO488–1,2-dipalmitoyl-*sn*-glycero-3-phosphoethanol-amine (ATTO-488-DPPE), was used to label the lipid bilayers of the vesicle. Labeling the lipid allowed for separating vesicles to be tracked during fluorescent imaging. Antibody and ligand binding were used to determine the specific location where 5-HT_{1A} was bound to the membrane. In this instance, 5-HT_{1A} antibodies were labeled with rhodamine and bound with a fluorescent antagonist so that researchers could determine whether 5-HT_{1A} successfully merged with the membrane. Ligand binding only occurred when 5-HT_{1A} was present in the proper orientation, so it was used as a negative control to detect whether the protein misfolded. To track phase separation, fluorescent images were studied. It was determined that 5-HT_{1A} segregated into the liquid disordered phase. This study shows that the usage of GUVs allows for phase observation of proteins in membranes. It is possible to modify this process for other receptors to gain a better understanding of their phase in membranes.

3.3.3. Charged proteoliposomes—In addition to single protein assembly, it is possible to assemble multiple sets of membrane protein complexes. One such method is through the fusion of charged proteoliposomes. This method has been used to reconstitute two different detergent-solubilized membrane protein complexes into charged small unilamellar vesicles (SUV) and subsequently fusing them with oppositely charged bilayers (Ishmukhametov et al., 2016). Specifically, *E. coli* F_1F_0 ATP-synthase and bo_3-oxidase were

used with the goal of forming an electron transport chain that can synthesize ATP. Similarly, Biner et al. used charge-mediated fusion to reconstitute bo_3-oxidase and ATP synthase into liposomes (Biner et al., 2016). Both methods are built off the basis of fusing differently charged proteoliposomes to build an electron transport chain (Fig. 5A).

For the fusion of the vesicles to occur, different lipid compositions were designed that fuse when mixed. The lipid compositions and ionic strength of the medium were altered to produce membrane proteins that retain their function. The vesicle fusion process was sensitive to membrane charge. Hence, the effect of the bilayer's charge on ATP-synthase and bo_3-oxidase was tested by reconstituting the proteins in cationic, anionic, and neutral proteoliposomes. It was determined that anionic SUVs produced the best result. The process of protein purification and reconstitution into SUVs was done by tagging F_1F_0 ATP-synthase and bo_3-oxidase with histidine and subsequently expressing them in DK-8 and C43(DE3) *E. coli* strains (Ishmukhametov et al., 2016). Following this, the proteins were purified and subsequently reconstituted in SUV by mixing the protein, extraction buffer, sodium cholate, SUVs, and buffer.

To build an electron transport chain, the vesicles were fused by combining positively charged proteoliposomes containing ATP-synthase and negatively charged proteoliposomes containing bo_3-oxidase (Ishmukhametov et al., 2016). They were fused in a mixture of KCl, MOPS, and $MgCl_2$. It was also shown that fusion could be done by using empty negatively charged GUVs with a separately prepared positively charged proteoliposome containing ATP-synthase or bo_3-oxidase. The luciferin-luciferase system was used to check whether the assembled electron transport chain produced luminescence. The luminescence assay demonstrated that ATP synthesis was occurring, and the proteins were fully functionalized.

3.3.4. SNARE-mediated vesicle fusion—Similar to the fusion of charged proteoliposomes, SNARE protein-mediated vesicle fusion has been used to deliver membrane proteins into bilayers. SNARE fusion takes longer than the method above, and SNARE is limited to small vesicles (Ishmukhametov et al., 2016). However, SNARE does not require lipid vesicles to be mixed in low ionic strength media, unlike the charged proteoliposome method.

SNARE fusion is based on the approach of using purified SNARE proteins to combine reconstituted membrane proteins in artificial and native membranes (Nordlund et al., 2014). This was done by separately reconstituting proteins in liposomes and then fusing the vesicles to create a vesicle containing multiple membrane proteins. After membrane protein reconstitution, vesicle- and target-SNARE proteins were added into the liposomes. Fusion was driven by the energy created by the v- and t-SNARE proteins interaction. This interaction brought the membranes of the vesicles to close together. Fusion into one large vesicle occurred due to the opening of membrane pores.

This method was used to reconstitute three membrane proteins: fumarate reductase, ATP synthase, and bo_3-oxidase (Nordlund et al., 2014) (Fig. 5B). Fumarate reductase was purified and reconstituted in vesicles containing v-SNARE synaptobrevin and ubiquinol Q_{10}, a lipid-soluble electron donor. ATP synthase and bo_3-oxidase were reconstituted in a vesicle

containing t-SNARE SNAP-25/syntaxin and ubiquinol Q_{10}. Similar to the proteoliposome method (in Section 3.3.3), ATP synthesis was determined by luciferin-luciferase. The synthesis of ATP can be interpreted as the formation of an intact membrane bilayer in which the membrane proteins retained the correct orientation.

This method can be altered by changing the SNARE proteins that are used to create multiple consecutive fusion processes. In doing so, it becomes possible to create larger multiprotein complexes. However, GUVs are preferable to combine more complexes. Since this process only works for SUVs, it would be interesting to combine SNARE proteins with charged proteoliposomes that can work in GUVs. This combination could broaden the way in which multiprotein complexes are assembled.

3.3.5. Purified proteins on liposomes—Enzymatic networks have also been assembled on unilamellar liposomes that mimic the natural membrane environment. It has been used to reconstitute the T cell receptor proximal signaling network, which is composed of Lck, tyrosine phosphatase CD45, Csk, and TCR subunit (CD3ζ) (Hui and Vale, 2014) (Fig. 5C). This network was reconstituted step by step by breaking it up into reactions relating to kinase or phosphatase. Then these components were recombined to create a fully formed network.

To build the network, Lck and CD3ζ were reconstituted on artificial lipid bilayers (Hui and Vale, 2014). For the binding of Lck to liposomes containing DGS-NTA-Ni lipids, its N-terminal glycine was replaced with a His_{10} tag; CD3ζ also had a His_{10} tag attached to it via Quikchange mutagenesis on its cytosolic domain. The protein product was labeled by inserting a Lys-Cys-Lys-Lys sequence between His_{10} and CD3ζ. To determine whether CD3ζ was phosphorylated, fluorescently labeled $SNAP_{505}$-tSH2 was utilized. To determine dephosphorylation rates of various forms of Lck, a recombinant cytoplasmic portion of CD45 was introduced to the system. Similarly, Csk was bound to the membrane to determine what phosphorylation effects it has to the Lck-CD3ζ.

This system relies on slowly combining enzymes with the liposomal membrane to determine how the system reacts. This strategy provides the researcher with information regarding the processes involved in the signaling network and what specifically affects the network. This methodology can be applied to reconstruct other signaling networks in a piece-by-piece manner. During the reconstruction process, researchers can also gather information regarding enzyme regulation as well as how the signaling system behaves like a network.

Similar to the reconstitution of the T cell receptor proximal signaling network, LAT-nucleated multiprotein signaling complexes have been reconstituted in liposomes by taking advantage of the membrane lipid bilayer. For this method, phosphotyrosine (PiY) was necessary as it recruited cytoplasmic signaling protein complexes (Sangani et al., 2009). When LAT, a type III transmembrane adaptor protein, is activated by TCR and FcεRI, it becomes tyrosine phosphorylated. Subsequently, SH2 domain-containing signaling proteins bind to LAT phosphotyrosines and further attract cytosolic protein partners like SLP76, Itk-1, Vav-1, Sos-1, and c-Cbl through SH3 domain interactions. This interaction also brings about additional intermolecular tyrosine phosphorylation.

For the reconstitution of myr/palm LAT in LUVs, phospholipids DOPS, DOPC, and DOPE had to undergo processing (Sangani et al., 2009). This processing consisted of introducing the lipids to chloroform, drying under nitrogen, and subsequently hydrating in degassed TBS buffer. Following this, the mixture formed LUVs by the extrusion method, then mixed with freshly purified myr/palm-LAT and 0.5% OG to produce LAT proteoliposomes. Subsequently, the LAT proteliposome had a tyrosine phosphorylated recombinant variant of the transmembrane adaptor protein Linker for Activation of T cells (PiYLAT) anchored to it via an N-terminal Lck anchor produced via acylation. PiYLAT proteoliposomes then recruited signaling protein complexes when incubated with Jurkat cytosol. These protein complexes were attached via LAT-binding proteins rather than directly to PiYLAT. Subsequently, nucleation occurred when in the presence of phosphatidylserine.

Overall, this mechanism relies on a liposomal membrane, which can be used to construct a signaling complex from the bottom up in a step-by-step manner. By reconstituting the LAT protein in LUVs, further proteins are recruited by way of a specific pattern to create the LAT-nucleated multiprotein signaling complex. This methodology can be further used in understanding as well as reconstituting membrane-based signaling networks.

3.4. Verification of proper protein-network reconstitution

Every method outlined above requires a test to determine whether the protein and protein networks have been properly reconstituted. For example, a luciferin-luciferase system was used to detect whether an electron transport chain remained functional following reconstitution (Nordlund et al., 2014). The synthesis of ATP represented the reconstitution of an intact protein network in which the membrane proteins retained the correct orientation (Ishmukhametov et al., 2016; Nordlund et al., 2014). For both the reconstitution of T cell receptor proximal signaling network and the reconstitution of LAT-nucleated multiprotein signaling complexes, their functions were tested by determining whether the signaling system behaved properly (Hui and Vale, 2014; Sangani et al., 2009). In addition to the aforementioned functional test, there were other direct ways to determine if proteins were properly reconstituted.

Electron crystallography has been widely used in the 2D imaging of membrane proteins, where proteins are packed together into a highly ordered crystallized sample (Raunser and Walz, 2009). Recently, cryo electron tomography (Cryo-ET) and subtomogram averaging (STA) have enabled the 3D characterization of proteins in aqueous environments, which can be used to determine the structure of individual non-crystalline membrane proteins in lipid membranes and whether a protein has been properly reconstituted. This method relied on analyzing how membrane proteins reacted to voltage and ligand gating. For instance, to confirm reconstructed mouse serotonin 5-HT_3 receptors in lipid vesicles, cryo-ET was performed with direct electron detection to obtain high-resolution structures of the membrane protein analyzed by STA. This process disclosed the receptors' secondary structural elements and gating mechanism, determined its position in the membrane, and demonstrated how interactions between densely packed receptors occurred (Kudryashev et al., 2016). This procedure can be used to study any membrane proteins and gated ion channels in lipid vesicles. Following self-assembly, newly formed complexes can undergo

cryo-ET for researchers to gain a better understanding of the structures that were created (Kudryashev et al., 2016). For example, cryo-ET can be used on the OmpF protein-vesicle complex created by photo-PISA to see exactly where the channel protein was incorporated and how it affected the structure.

The basis of this method is to structurally analyze large soluble proteins by performing single-particle reconstruction from electron microscopy of cryogenically cooled samples (cryo-EM). Similar to cryo-ET, this method images membrane proteins in a lipid environment (Wang and Sigworth, 2009). For instance, this procedure was performed with reconstituted BK potassium channels in liposomes. Reconstitution was performed by Flag-tagging the human gene SLO to extract membrane proteins and subsequently purify with an anti-Flag affinity column. The reconstituted vesicles were then frozen and imaged to obtain a 1.7–2.0 nm resolution 3D reconstruction of the channel and the membrane, within which was enclosed. To make sure that the BK channels were still functional following reconstitution, a fluorescent dye was used to monitor changes in the membrane potential caused by fluctuating potassium ion concentrations. This is yet another imaging process that allows for self-assembled membrane structures and their function to be further analyzed. It differs from cryo-ET because it allows for the channel's activity to also be assayed. However, this method is controversial as some believe that the embedded channel's VSDs do not match 6TM channel X-ray crystal structures (Wang and Sigworth, 2009).

4. Conclusion

Bottom-up construction of protein networks may benefit from standardized strategies and protocols. Such standardized strategies may facilitate the precise assembling of individual components. For instance, the traditional membrane assembly methods (e.g., centrifuge, extrusion, film hydration) lack precise control over vesicle size, content, and membrane compositions. The community also currently lacks a mechanistic understanding of the protein-network assembly due to the difficulty of in-depth characterizations (Swank et al., 2019) and various confounding effects (Laohakunakorn et al., 2020). Characterizing the function of each protein component in the whole network is a challenging task. Several effects may confound the proper folding and functioning of a protein, including i) upon the self-assembly of core protein domains into a synthetic system (i.e., liposome or water-in-oil droplet), the membrane may allow nonspecific surfactant adsorption when smaller surfactants (i.e., Span 80) are used (Abu Shah et al., 2015), or bring bilayer's charge effect (Sangani et al., 2009) on membrane proteins. ii) directional orientation of proteins can affect their function (Hagan et al., 2010; Nordlund et al., 2014). iii) distribution of protein concentrations and composition can affect the function of a protein network (Nordlund et al., 2014). Thus, precision control is required to assemble and confirm individual components of a complex network (Miller et al., 2020). In addition, precision control is critical for the optimization of protein networks that is indispensable to enhance the function of protein networks.

In addition, the current high cost of producing recombinant proteins in large amounts (Feinberg and Parker, 2010) and automated equipment (Villarreal et al., 2018) prohibits a wide-spread study of protein-networks in synthetic systems. The crucial step to build a

protein network is to obtain high-quality proteins. Hence, the natural properties of proteins should not be altered when they undergo the entire process of protein expression and extraction. However, it is broadly known that protein properties can change due to culturing conditions such as the degree of aeration, the cultural growth size, and temperature. Furthermore, the property of inserted protein tag (i.e., amino acid length, dimer) and the N or C terminal-tagging also affects the folding of a protein (Gräslund et al., 2008). To check for these effects, the purified proteins must be characterized by mass spectrometry and gel electro-phoresis (Gräslund et al., 2008). The protein purification also requires multiple labor-intensive steps that lead to a high cost. Although automated multiprotein purification is currently available (Camper and Viola, 2009), we still need to optimize the protocols for each protein due to their diverse properties. To overcome the tedious optimization steps, machine learning (Habibi et al., 2014) and standardized protocols (Sjöstrand et al., 2017) may be used to predict and speed up the individual steps. Furthermore, for initial exploratory studies, cell-free systems could be used to speed up the synthesis of multiple proteins (Contreras-Llano et al., 2020).

While droplet-based microfluidic devices have been widely used in the formation of LUV and GUV, it requires further technological innovations to enable the multiplexing of proteins in vesicles (Shembekar et al., 2016). For example, a membrane protein could be varied at particular orientations or folding structures to examine its impact on the function of a protein network. The associated challenge is to further manipulate preformed LUVs and GUVs by maintaining their permeability and mechanical instability in their interactions with a broad range of extracellular matrices, cells, and signaling proteins (Jørgensen et al., 2017). In addition, when conducting multifactorial experiments, it remains challenging to screen a complex protein network where tens or even hundreds of variables are involved, such as a complete MAPK signaling pathway (Rasmussen et al., 2012). In this case, parts of a complex protein network could be screened with a standard method, and then rationally assembled without an extensive large screen (Swank et al., 2019). Meanwhile, computational models of a protein network might provide a complementary tool to narrow down the dynamic range of a complex system. Moreover, auto-generation of the membrane is an unsolved task in synthetic systems. Bhattacharya et al. (Bhattacharya et al., 2019) demonstrated a simplified method of phospholipid self-synthesis that requires FadD10 (fatty-acid-CoA synthetase) and a continuous supplement of fresh reactive precursors. This work opens the door for generating and maintaining phospholipid membranes in synthetic systems.

In summary, there is a renaissance in the assembly of protein networks for various novel applications, such as switch ON/OFF signaling pathways and sensing environments through membrane proteins. We envision that a multi-disciplinary approach could alleviate the current challenges of constructing complex protein networks from the bottom-up. Such efforts will also pave the way to construct and study protein networks in a high-throughput way. The positive feedback loop between basic studies and construction technology of protein networks may one day broaden the application of synthetic protein networks for drug delivery, drug screening, biosensors, metabolic engineering, dynamic research tools, and tissue engineering.

Acknowledgements

The work is supported by NIH (5R21EB025938).

References

Abate AR, Hung T, Mary P, Agresti JJ, Weitz DA, 2010. High-throughput injection with microfluidics using picoinjectors. Proc. Natl. Acad. Sci 10.1073/pnas.1006888107.

Abu Shah E, Keren K, 2014. Symmetry breaking in reconstituted actin cortices. Elife. 10.7554/elife.01433.

Abu Shah E, Malik-Garbi M, Keren K, 2015. Reconstitution of cortical actin networks within water-in-oil emulsions. Methods Cell Biol. 10.1016/bs.mcb.2015.01.011.

Adamala KP, Martin-Alarcon DA, Guthrie-Honea KR, Boyden ES, 2017. Engineering genetic circuit interactions within and between synthetic minimal cells. Nat. Chem 10.1038/nchem.2644.

Bally M, Bailey K, Sugihara K, Grieshaber D, Vörös J, Städler B, 2010. Liposome and lipid bilayer arrays towards biosensing applications. Small. 10.1002/smll.201000644.

Becker W, Scherer A, Faust C, Bauer DK, Scholtes S, Rao E, Hofmann J, Schauder R, Langer T, 2019. A fully automated three-step protein purification procedure for up to five samples using the NGC chromatography system. Protein Expr. Purif 10.1016/j.pep.2018.08.003.

Berhanu S, Ueda T, Kuruma Y, 2019. Artificial photosynthetic cell producing energy for protein synthesis. Nat. Commun 10.1038/s41467-019-09147-4.

Bhattacharya A, Brea RJ, Niederholtmeyer H, Devaraj NK, 2019. A minimal biochemical route towards de novo formation of synthetic phospholipid membranes. Nat. Commun 10.1038/s41467-018-08174-x.

Biner O, Schick T, Müller Y, von Ballmoos C, 2016. Delivery of membrane proteins into small and giant unilamellar vesicles by charge-mediated fusion. FEBS Lett. 10.1002/1873-3468.12233.

Brizzard BL, Chubet RG, Vizard DL, 1994. Immunoaffinity purification of FLAG® epitope-tagged bacterial alkaline phosphatase using a novel monoclonal antibody and peptide elution. Biotechniques.

Buck M, Gallegos MT, Studholme DJ, Guo Y, Gralla JD, 2000. The bacterial enhancer-dependent σ54 (σ(N)) transcription factor. J. Bacteriol 10.1128/JB.182.15.4129-4136.2000.

Camper DMV, Viola RE, 2009. Fully automated protein purification. Anal. Biochem 10.1016/j.ab.2009.07.009.

Contreras-Llano LE, Meyer C, Liu Y, Sarker M, Lim S, Longo ML, Tan C, 2020. Holistic engineering of cell-free systems through proteome-reprogramming synthetic circuits. Nat. Commun 11 10.1038/s41467-020-16900-7.

Cui N, Zhang H, Schneider N, Tao Y, Asahara H, Sun Z, Cai Y, Koehler SA, De Greef TFA, Abbaspourrad A, Weitz DA, Chong S, 2016. A mix-and-read drop-based *in vitro* two-hybrid method for screening high-affinity peptide binders. Sci. Rep 10.1038/srep22575.

di Guana C, Lib P, Riggsa PD, Inouyeb H, 1988. Vectors that facilitate the expression and purification of foreign peptides in *Escherichia coli* by fusion to maltose-binding protein. Gene. 10.1016/0378-1119(88)90004-2.

Ding Y, Huang E, Lam KS, Pan T, 2013. Microfluidic impact printer with interchangeable cartridges for versatile non-contact multiplexed micropatterning. Lab Chip 13, 1902–1910. 10.1039/c3lc41372a. [PubMed: 23525299]

Ding Y, Contreras-Llano LE, Morris E, Mao M, Tan C, 2018. Minimizing context dependency of gene networks using artificial cells. ACS Appl. Mater. Interfaces 10.1021/acsami.8b10029.

Dueber JE, Wu GC, Malmirchegini GR, Moon TS, Petzold CJ, Ullal AV, Prather KLJ, Keasling JD, 2009. Synthetic protein scaffolds provide modular control over metabolic flux. Nat. Biotechnol 10.1038/nbt.1557.

Dürre K, Keber FC, Bleicher P, Brauns F, Cyron CJ, Faix J, Bausch AR, 2018. Capping protein-controlled actin polymerization shapes lipid membranes. Nat. Commun 10.1038/s41467-018-03918-1.

Fan J, Villarreal F, Weyers B, Ding Y, Tseng KH, Li J, Li B, Tan C, Pan T, 2017. Multi-dimensional studies of synthetic genetic promoters enabled by microfluidic impact printing. Lab Chip 17, 2198–2207. 10.1039/c7lc00382j. [PubMed: 28613297]

Fan J, Men Y, Hao Tseng K, Ding YY, Ding YY, Villarreal F, Tan C, Li B, Pan T, 2018. Dotette: programmable, high-precision, plug-and-play droplet pipetting. Biomicrofluidics 12. 10.1063/1.5030629.

Feinberg AW, Parker KK, 2010. Surface-initiated assembly of protein nanofabrics. Nano Lett. 10.1021/nl100998p.

Fujii S, Matsuura T, Sunami T, Kazuta Y, Yomo T, 2013. *In vitro* evolution of α-hemolysin using a liposome display. Proc. Natl. Acad. Sci. U. S. A 10.1073/pnas.1314585110.

Garamella J, Majumder S, Liu AP, Noireaux V, 2019. An adaptive synthetic cell based on mechanosensing, biosensing, and inducible gene circuits. ACS Synth. Biol. 10.1021/acssynbio.9b00204.

Gloeckner CJ, Boldt K, Schumacher A, Roepman R, Ueffing M, 2007. A novel tandem affinity purification strategy for the efficient isolation and characterisation of native protein complexes. Proteomics. 10.1002/pmic.200700038.

Godino E, López JN, Foschepoth D, Cleij C, Doerr A, Castellà CF, Danelon C, 2019. De novo synthesized Min proteins drive oscillatory liposome deformation and regulate FtsA-FtsZ cytoskeletal patterns. Nat. Commun 10.1038/s41467-019-12932-w.

Gräslund S, Nordlund P, Weigelt J, Hallberg BM, Bray J, Gileadi O, Knapp S, Oppermann U, Arrowsmith C, Hui R, Ming J, dhe-Paganon S, Park HW, Savchenko A, Yee A, Edwards A, Vincentelli R, Cambillau C, Kim R, Kim SH, Rao Z, Shi Y, Terwilliger TC, Kim CY, Hung LW, Waldo GS, Peleg Y, Albeck S, Unger T, Dym O, Prilusky J, Sussman JL, Stevens RC, Lesley SA, Wilson IA, Joachimiak A, Collart F, Dementieva I, Donnelly MI, Eschenfeldt WH, Kim Y, Stols L, Wu R, Zhou M, Burley SK, Emtage JS, Sauder JM, Thompson D, Bain K, Luz J, Gheyi T, Zhang F, Atwell S, Almo SC, Bonanno JB, Fiser A, Swaminathan S, Studier FW, Chance MR, Sali A, Acton TB, Xiao R, Zhao L, Ma LC, Hunt JF, Tong L, Cunningham K, Inouye M, Anderson S, Janjua H, Shastry R, Ho CK, Wang D, Wang H, Jiang M, Montelione GT, Stuart DI, Owens RJ, Daenke S, Schütz A, Heinemann U, Yokoyama S, Büssow K, Gunsalus KC, 2008. Protein production and purification. Nat. Methods 5, 135–146. 10.1038/nmeth.f.202. [PubMed: 18235434]

Gutierrez MG, Malmstadt N, 2014. Human serotonin receptor 5-HT1Apreferentially segregates to the liquid disordered phase in synthetic lipid bilayers. J. Am. Chem. Soc 10.1021/ja507221m.

Habibi N, Mohd Hashim SZ, Norouzi A, Samian MR, 2014. A review of machine learning methods to predict the solubility of overexpressed recombinant proteins in *Escherichia coli*. BMC Bioinformatics 15. 10.1186/1471-2105-15-134.

Hadimioglu B, Stearns R, Ellson R, 2016. Moving liquids with sound: the physics of acoustic droplet ejection for robust laboratory automation in life sciences. J. Lab. Autom 10.1177/2211068215615096.

Hagan CL, Kim S, Kahne D, 2010. Reconstitution of outer membrane protein assembly from purified components. Science (80-.). 10.1126/science.1188919.

Hahn A, Vonck J, Mills DJ, Meier T, Kühlbrandt W, 2018. Structure, mechanism, and regulation of the chloroplast ATP synthase. Science (80-.). 10.1126/science.aat4318.

Hammerling MJ, Fritz BR, Yoesep DJ, Kim DS, Carlson ED, Jewett MC, 2020. *In vitro* ribosome synthesis and evolution through ribosome display. Nat. Commun 10.1038/s41467-020-14705-2.

Hindley JW, Zheleva DG, Elani Y, Charalambous K, Barter LMC, Booth PJ, Bevan CL, Law RV, Ces O, 2019. Building a synthetic mechanosensitive signaling pathway in compartmentalized artificial cells. Proc. Natl. Acad. Sci. U. S. A 10.1073/pnas.1903500116.

Hochuli E, Döbeli H, Schacher A, 1987. New metal chelate adsorbent selective for proteins and peptides containing neighbouring histidine residues. J. Chromatogr. A 10.1016/S0021-9673(00)93969-4.

Hu J, Qin H, Sharma M, Cross TA, Gao FP, 2008. Chemical cleavage of fusion proteins for high-level production of transmembrane peptides and protein domains containing conserved methionines. Biochim. Biophys. Acta Biomembr 10.1016/j.bbamem.2007.12.024.

Huang WYC, Yan Q, Lin WC, Chung JK, Hansen SD, Christensen SM, Tu HL, Kuriyan J, Groves JT, 2016. Phosphotyrosine-mediated LAT assembly on membranes drives kinetic bifurcation in recruitment dynamics of the Ras activator SOS. Proc. Natl. Acad. Sci. U. S. A 10.1073/pnas.1602602113.

Hui E, Vale RD, 2014. *In vitro* membrane reconstitution of the T-cell receptor proximal signaling network. Nat. Struct. Mol. Biol 10.1038/nsmb.2762.

Ishmukhametov RR, Russell AN, Berry RM, 2016. A modular platform for one-step assembly of multi-component membrane systems by fusion of charged proteoliposomes. Nat. Commun 10.1038/ncomms13025.

Jewett MC, Fritz BR, Timmerman LE, Church GM, 2013. *In vitro* integration of ribosomal RNA synthesis, ribosome assembly, and translation. Mol. Syst. Biol 10.1038/msb.2013.31.

Jones RB, Gordus A, Krall JA, MacBeath G, 2006. A quantitative protein interaction network for the ErbB receptors using protein microarrays. Nature. 10.1038/nature04177.

Jørgensen IL, Kemmer GC, Pomorski TG, 2017. Membrane protein reconstitution into giant unilamellar vesicles: a review on current techniques. Eur. Biophys. J 10.1007/s00249-016-1155-9.

Kimple ME, Sondek J, 2002. Affinity tag for protein purification and detection based on the disulfide-linked complex of InaD and NorpA. Biotechniques. 10.2144/02333rr01.

Kimple ME, Brill AL, Pasker RL, 2013. Overview of affinity tags for protein purification. Curr. Protoc. Protein Sci 10.1002/0471140864.ps0909s73.

Köster DV, Husain K, Iljazi E, Bhat A, Bieling P, Mullins RD, Rao M, Mayor S, 2016. Actomyosin dynamics drive local membrane component organization in an *in vitro* active composite layer. Proc. Natl. Acad. Sci. U. S. A 10.1073/pnas.1514030113.

Kudryashev M, Castaño-Díez D, Deluz C, Hassaine G, Grasso L, Graf-Meyer A, Vogel H, Stahlberg H, 2016. The structure of the mouse serotonin 5-HT3 receptor in lipid vesicles. Structure. 10.1016/j.str.2015.11.004.

Lalo H, Cau JC, Thibault C, Marsaud N, Severac C, Vieu C, 2009. Microscale multiple biomolecules printing in one step using a PDMS macrostamp. Microelectron. Eng 10.1016/j.mee.2008.11.088.

Laohakunakorn N, Grasemann L, Lavickova B, Michielin G, Shahein A, Swank Z, Maerkl SJ, 2020. Bottom-up construction of complex biomolecular systems with cell-free synthetic biology. Front. Bioeng. Biotechnol 10.3389/fbioe2020.00213.

Lee KY, Park SJ, Lee KA, Kim SH, Kim H, Meroz Y, Mahadevan L, Jung KH, Ahn TK, Parker KK, Shin K, 2018. Photosynthetic artificial organelles sustain and control ATP-dependent reactions in a protocellular system. Nat. Biotechnol 10.1038/nbt.4140.

Lenaerts T, Schymkowitz J, Rousseau F, 2009. Protein domains as information processing units. Curr. Protein Pept. Sci 10.2174/138920309787847626.

Lentini R, Santero SP, Chizzolini F, Cecchi D, Fontana J, Marchioretto M, Del Bianco C, Terrell JL, Spencer AC, Martini L, Forlin M, Assfalg M, Serra MD, Bentley WE, Mansy SS, 2014. Integrating artificial with natural cells to translate chemical messages that direct *E. coli* behaviour. Nat. Commun 10.1038/ncomms5012.

Lentini R, Martín NY, Forlin M, Belmonte L, Fontana J, Cornella M, Martini L, Tamburini S, Bentley WE, Jousson O, Mansy SS, 2017. Two-way chemical communication between artificial and natural cells. ACS Cent. Sci 10.1021/acscentsci.6b00330.

Li B, Fan J, Li J, Chu J, Pan T, 2015. Piezoelectric-driven droplet impact printing with an interchangeable microfluidic cartridge. Biomicrofluidics 9, 1–11. 10.1063/1.4928298.

Li J, Tan W, Xiao W, Carney RP, Men Y, Li Y, Quon G, Ajena Y, Lam KS, Pan T, 2018. A plug-and-play, drug-on-pillar platform for combination drug screening implemented by microfluidic adaptive printing. Anal. Chem 10.1021/acs.analchem.8b03456.

Lichty JJ, Malecki JL, Agnew HD, Michelson-Horowitz DJ, Tan S, 2005. Comparison of affinity tags for protein purification. Protein Expr. Purif 10.1016/j.pep.2005.01.019.

Liu Z, Cao S, Liu M, Kang W, Xia J, 2019. Self-assembled multienzyme nanostructures on synthetic protein scaffolds. ACS Nano. 10.1021/acsnano.9b04554.

Ma C, Hao Z, Huysmans G, Lesiuk A, Bullough P, Wang Y, Bartlam M, Phillips SE, Young JD, Goldman A, Baldwin SA, Postis VLG, 2015. A versatile strategy for production of membrane

proteins with diverse topologies: application to investigation of bacterial homologues of human divalent metal ion and nucleoside transporters. PLoS One. 10.1371/journal.pone.0143010.

MacBeath G, Schreiber SL, 2000. Printing proteins as microarrays for high-throughput function determination. Science. 10.1126/science.289.5485.1760.

Maerkl SJ, Quake SR, 2007. A systems approach to measuring the binding energy landscapes of transcription factors. Science (80-.). 10.1126/science.1131007.

Matsubayashi H, Kuruma Y, Ueda T, 2014. *In vitro* synthesis of the *E. coli* sec translocon from DNA. Angew. Chem. Int. Ed 10.1002/anie.201403929.

Miller TE, Beneyton T, Schwander T, Diehl C, Girault M, Mclean R, Chotel T, Claus P, Cortina NS, Baret J, Erb TJ, 2020. Light-Powered CO_2 Fixation in a Chloroplast Mimic with Natural and Synthetic Parts 654, pp. 649–654.

Milo R, 2013. What is the total number of protein molecules per cell volume? A call to rethink some published values. BioEssays. 10.1002/bies.201300066.

Mittendorf KF, Marinko JT, Hampton CM, Ke Z, Hadziselimovic A, Schlebach JP, Law CL, Li J, Wright ER, Sanders CR, Ohi MD, 2017. Peripheral myelin protein 22 alters membrane architecture. Sci. Adv 10.1126/sciadv.1700220.

Monsey J, Shen W, Schlesinger P, Bose R, 2010. Her4 and Her2/neu tyrosine kinase domains dimerize and activate in a reconstituted *in vitro* system. J. Biol. Chem 10.1074/jbc.M109.096032.

Moon TS, Dueber JE, Shiue E, Prather KLJ, 2010. Use of modular, synthetic scaffolds for improved production of glucaric acid in engineered *E. coli*. Metab. Eng 10.1016/j.ymben.2010.01.003.

Moore SJ, MacDonald JT, Wienecke S, Ishwarbhai A, Tsipa A, Aw R, Kylilis N, Bell DJ, McClymont DW, Jensen K, Polizzi KM, Biedendieck R, Freemont PS, 2018. Rapid acquisition and model-based analysis of cell-free transcription–translation reactions from nonmodel bacteria. Proc. Natl. Acad. Sci. U. S. A 10.1073/pnas.1715806115.

Moritani Y, Nomura SIM, Morita I, Akiyoshi K, 2010. Direct integration of cell-free-synthesized connexin-43 into liposomes and hemichannel formation. FEBS J. 10.1111/j.1742-4658.2010.07736.x.

Müller UR, Papen R, 2005. Manufacturing of 2-D Arrays by Pin-Printing Technologies. 10.1007/3-540-26578-3_5.

Noireaux V, Libchaber A, 2004. A vesicle bioreactor as a step toward an artificial cell assembly. Proc. Natl. Acad. Sci. U. S. A 10.1073/pnas.0408236101.

Nomura S, Ichiro M, Kondoh S, Asayama W, Asada A, Nishikawa S, Akiyoshi K, 2008. Direct preparation of giant proteo-liposomes by *in vitro* membrane protein synthesis. J. Biotechnol 10.1016/j.jbiotec.2007.08.023.

Nordlund G, Brzezinski P, Von Ballmoos C, 2014. SNARE-fusion mediated insertion of membrane proteins into native and artificial membranes. Nat. Commun 10.1038/ncomms5303.

Palchesko RN, Funderburgh JL, Feinberg AW, 2016. Engineered basement membranes for regenerating the corneal endothelium. Adv. Healthc. Mater 10.1002/adhm.201600488.

Quick M, Wright EM, 2002. Employing *Escherichia coli* to functionally express, purify, and characterize a human transporter. Proc. Natl. Acad. Sci. U. S. A 10.1073/pnas.132266599.

Rafelski SM, Theriot JA, 2004. Crawling toward a unified model of cell motility: spatial and temporal regulation of actin dynamics. Annu. Rev. Biochem.s 10.1146/annurev.biochem.73.011303.073844.

Rahman M, Ismat F, McPherson MJJ, Baldwin SA, 2007. Topology-informed strategies for the overexpression and purification of membrane proteins. Mol. Membr. Biol 10.1080/09687860701243998.

Rampioni G, D'Angelo F, Messina M, Zennaro A, Kuruma Y, Tofani D, Leoni L, Stano P, 2018. Synthetic cells produce a quorum sensing chemical signal perceived by: *Pseudomonas aeruginosa*. Chem. Commun 10.1039/c7cc09678j.

Rasmussen MW, Roux M, Petersen M, Mundy J, 2012. MAP kinase cascades in *Arabidopsis* innate immunity. Front. Plant Sci 3, 1–6. 10.3389/fpls.2012.00169. [PubMed: 22645563]

Raunser S, Walz T, 2009. Electron crystallography as a technique to study the structure on membrane proteins in a lipidic environment. Annu. Rev. Biophys 10.1146/annurev.biophys.050708.133649.

Reymann AC, Boujemaa-Paterski R, Martiel JL, Guérin C, Cao W, Chin HF, De La Cruz EM, Théry M, Blanchoin L, 2012. Actin network architecture can determine myosin motor activity. Science (80-.). 10.1126/science.1221708.

Sangani D, Venien-Bryan C, Harder T, 2009. Phosphotyrosine-dependent *in vitro* reconstitution of recombinant LAT-nucleated multiprotein signalling complexes on liposomes. Mol. Membr. Biol 10.1080/09687680802637660.

Shembekar N, Chaipan C, Utharala R, Merten CA, 2016. Droplet-based microfluidics in drug discovery, transcriptomics and high-throughput molecular genetics. Lab Chip. 10.1039/c6lc00249h.

Sigrell JA, Eklund P, Galin M, Hedkvist L, Liljedahl P, Johansson CM, Pless T, Torstenson K, 2003. Automated multi-dimensional purification of tagged proteins. J. Struct. Funct. Genom 10.1023/A:1026202319763.

Sjöstrand D, Diamanti R, Lundgren CAK, Wiseman B, Högbom M, 2017. A rapid expression and purification condition screening protocol for membrane protein structural biology. Protein Sci. 26, 1653–1666. 10.1002/pro.3196. [PubMed: 28543736]

Smith DB, Johnson KS, 1988. Single-step purification of polypeptides expressed in *Escherichia coli* as fusions with glutathione S-transferase. Gene. 10.1016/0378-1119(88)90005-4.

Stano P, 2019. Gene expression inside liposomes: from early studies to current protocols. Chem. - A Eur. J 10.1002/chem.201806445.

Stearns DJ, Kurosawa S, Sims PJ, Esmon NL, Esmon CT, 1988. The interaction of a Ca^{2+-}dependent monoclonal antibody with the protein C activation peptide reaction. Evidence for obligatory Ca^{2+} binding to both antigen and antibody. J. Biol. Chem 10.1016/s0021-9258(19)35429-8.

Stofko-Hahn RE, Carr DW, Scott JD, 1992. A single step purification for recombinant proteins characterization of a microtubule associated protein (MAP 2) fragment which associates with the type II cAMP-dependent protein kinase. FEBS Lett. 10.1016/0014-5793(92)80458-S.

Su X, Ditlev JA, Hui E, Xing W, Banjade S, Okrut J, King DS, Taunton J, Rosen MK, Vale RD, 2016. Phase separation of signaling molecules promotes T cell receptor signal transduction. Science (80-.). 10.1126/science.aad9964.

Swank Z, Laohakunakorn N, Maerkl SJ, 2019. Cell-free gene-regulatory network engineering with synthetic transcription factors. Proc. Natl. Acad. Sci. U. S. A 10.1073/pnas.1816591116.

Tan C, Saurabh S, Bruchez MP, Schwartz R, Leduc P, 2013. Molecular crowding shapes gene expression in synthetic cellular nanosystems. Nat. Nanotechnol 10.1038/nnano.2013.132.

Varlas S, Blackman LD, Findlay HE, Reading E, Booth PJ, Gibson MI, O'Reilly RK, 2018. Photoinitiated polymerization-induced self-assembly in the presence of surfactants enables membrane protein incorporation into vesicles. Macromolecules. 10.1021/acs.macromol.8b00994.

Villarreal F, Contreras-Llano LE, Chavez M, Ding Y, Fan J, Pan T, Tan C, Contreras-Llano LE, Chavez M, Tan C, 2018. Synthetic microbial consortia enable rapid assembly of pure translation machinery. Nat. Chem. Biol 14, 29–35. 10.1038/nchembio.2514. [PubMed: 29131146]

Von Ballmoos C, Biner O, Nilsson T, Brzezinski P, 2016. Mimicking respiratory phosphorylation using purified enzymes. Biochim. Biophys. Acta Bioenerg 1857, 321–331. 10.1016/j.bbabio.2015.12.007.

Voss S, Skerra A, 1997. Mutagenesis of a flexible loop in streptavidin leads to higher affinity for the Strep-tag II peptide and improved performance in recombinant protein purification. Protein Eng. 10.1093/protein/10.8.975.

Wang L, Sigworth FJ, 2009. Structure of the BK potassium channel in a lipid membrane from electron cryomicroscopy. Nature. 10.1038/nature08291.

Wang J, Deng K, Zhou C, Fang Z, Meyer C, Deshpande KUA, Li Z, Mi X, Luo Q, Hammock BD, Tan C, Chen Y, Pan T, 2019. Microfluidic cap-To-dispense (μCD): A universal microfluidic-robotic interface for automated pipette-free high-precision liquid handling. Lab Chip. 10.1039/c9lc00622b.

Wang X, Liu X, Huang X, 2020. Bioinspired protein-based assembling: toward advanced life-like behaviors. Adv. Mater 10.1002/adma.202001436.

Weiss M, Frohnmayer JP, Benk LT, Haller B, Janiesch JW, Heitkamp T, Börsch M, Lira RB, Dimova R, Lipowsky R, Bodenschatz E, Baret JC, Vidakovic-Koch T, Sundmacher K, Platzman I, Spatz JP,

2018. Sequential bottom-up assembly of mechanically stabilized synthetic cells by microfluidics. Nat. Mater 10.1038/NMAT5005.

Zhang X, Gureasko J, Shen K, Cole PA, Kuriyan J, 2006. An allosteric mechanism for activation of the kinase domain of epidermal growth factor receptor. Cell. 10.1016/j.cell.2006.05.013.

Zhou Y, Asahara H, Schneider N, Dranchak P, Inglese J, Chong S, 2014. Engineering bacterial transcription regulation to create a synthetic *in vitro* two-hybrid system for protein interaction assays. J. Am. Chem. Soc 10.1021/ja502512g.

Zuo X, Li S, Hall J, Mattern MR, Tran H, Shoo J, Tan R, Weiss SR, Butt TR, 2005. Enhanced expression and purification of membrane proteins by SUMO fusion in *escherichia coli*. J. Struct. Funct. Genom 10.1007/s10969-005-2664-4.

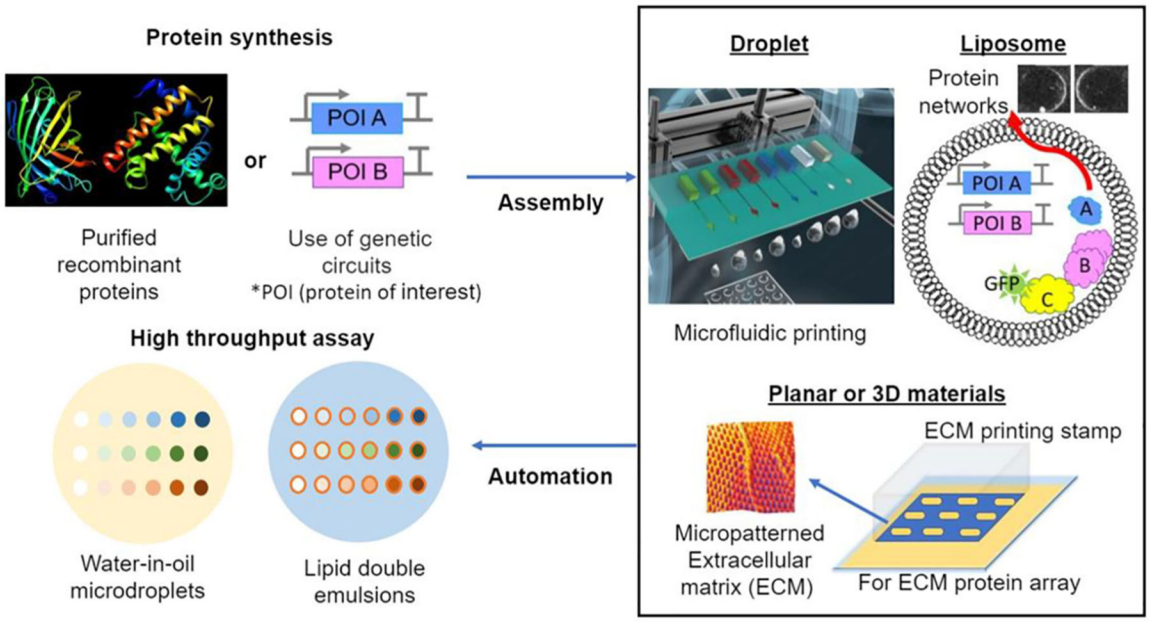

Fig. 1.

Schematic representation of the modern technologies for assembling protein networks in droplets, liposomes, and planar or 3D materials. The assembly of protein networks can be automated to enable high-throughput assays. Molecular graphics performed with UCSF (University of California, San Francisco) Chimera. Reproduced from (Godino et al., 2019) copyright 2019 The Author(s). Reprinted with permission from (Fan et al., 2017) copyright 2017 The Royal Society of Chemistry. Adapted with permission from (Feinberg and Parker, 2010). Copyright 2010 American Chemical Society.

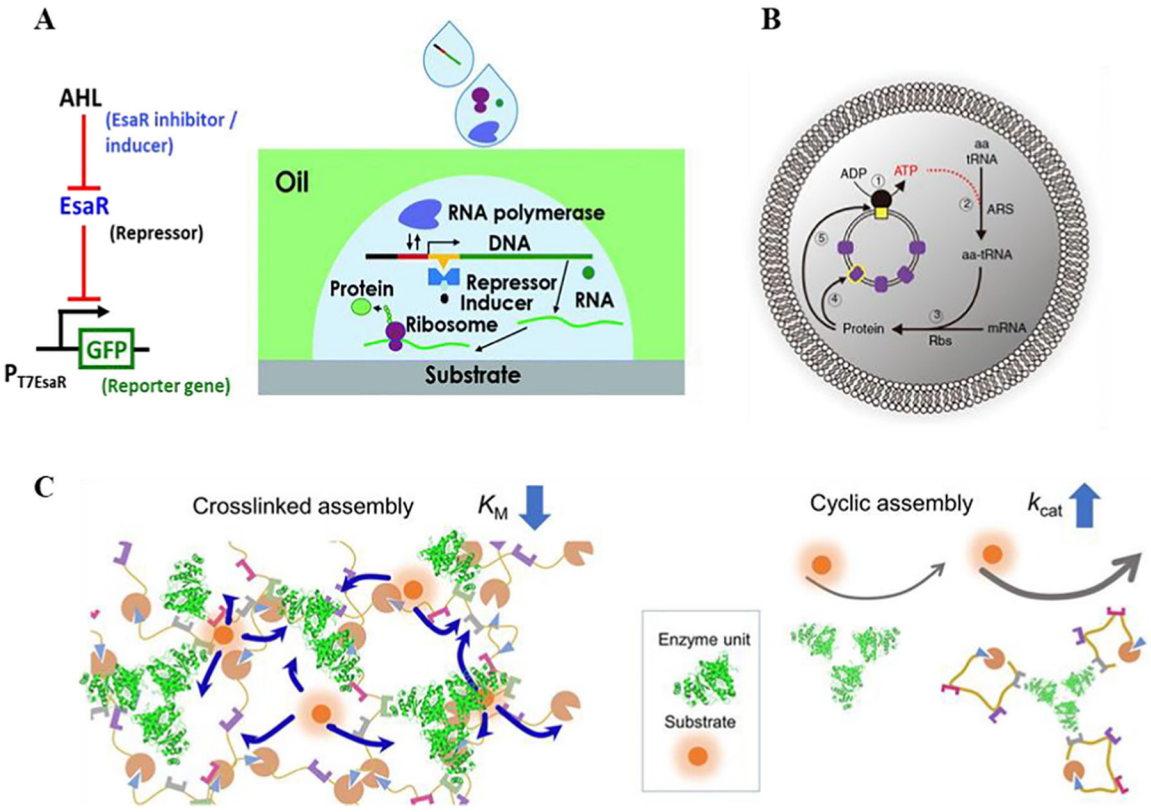

Fig. 2.

Synthetic protein networks in liposomes and water-in-oil droplets. (A) Illustration of the interactions of plasmids, repressor EsaR, and EsaR inhibitor AHL. Plasmids, EsaR, AHL, and the transcription–translation reaction mix were separately printed using a printer. Reprinted with permission from Fan et al. (2017) copyright 2017 The Royal Society of Chemistry. (B) Schematic of protein synthesis in artificial photosynthetic cells. Reprinted with permission from Berhanu et al. (2019). Copyright 2019, Springer Nature. (C) Illustration of the different protein scaffold assemblies and their influence on enzyme kinetics. Reprinted with permission from Liu et al. (2019). Copyright 2019 American Chemical Society.

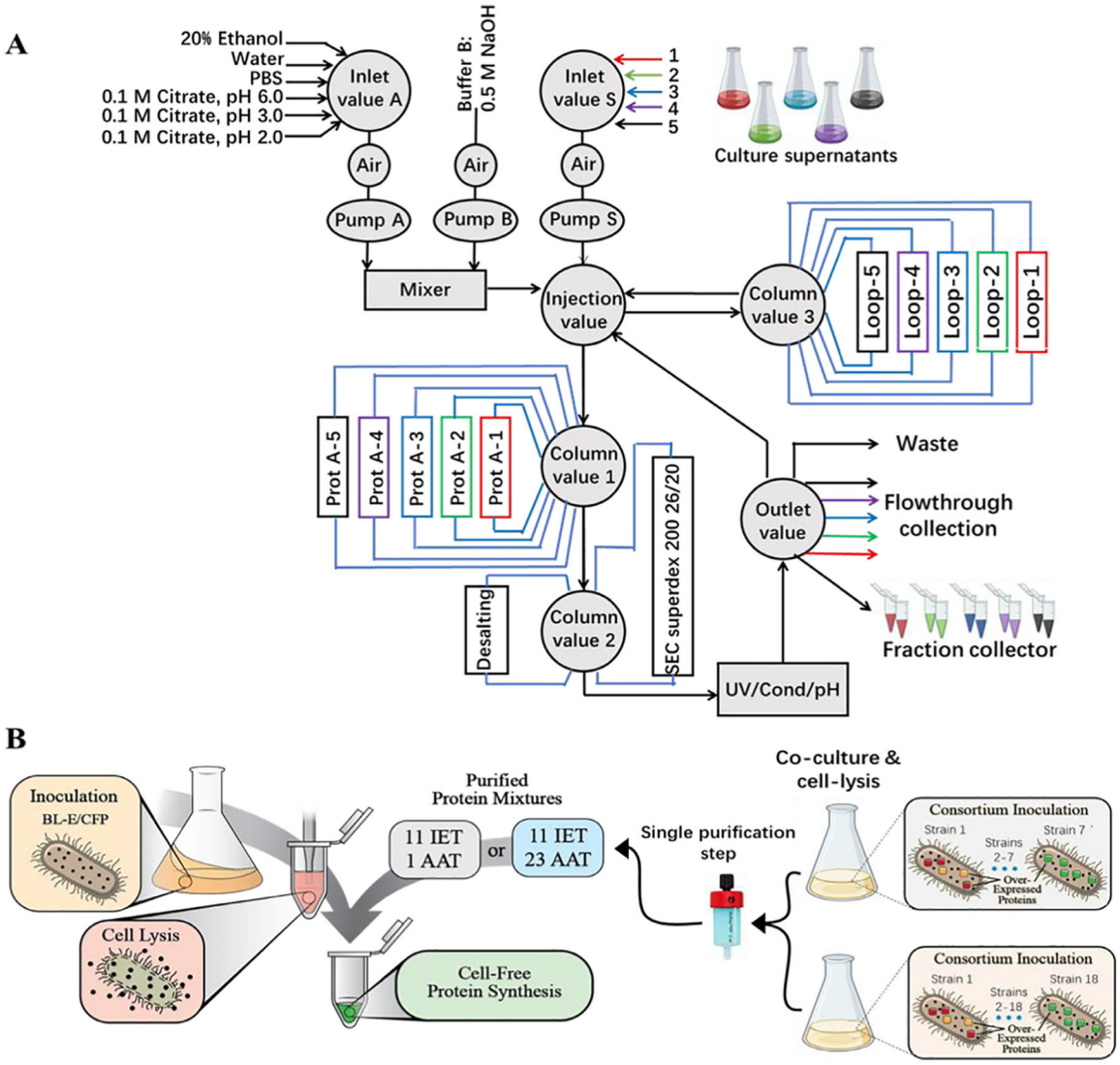

Fig. 3.

Schematic of two multiprotein purification platforms. (A) Schematic drawing of the sample flow. The samples are loaded through Inv–S, an air detector using the sample pump (Pump S) onto the Protein A columns. During sample loading, which is monitored via the UV-detector, the flow-through can be separately collected for each sample. Wash fractions are directed into the waste. Upon eluting protein from the Protein A column, the protein is then directed onto the desalting column and again passes the UV-detector. Samples are directed via the outlet valve (OV) and the Inj-V into the storage loops. From the storage loops, the samples are directed via the Inj-V to CV1 (in bypass-mode) and loaded via CV2 onto the size exclusion chromatography column. Again, samples pass the UV-detector. The fractions of interest are collected with the aid of a fraction collector. Reproduced from Becker et al. (2019) with copyright of Elsevier 2014 (B) Graphical representation of the supplementation of purified translation factors to CFPS reactions assembled using BL-E_{WCE} & BL-CFP_{WCE}. Two different mixtures of purified translation machinery were produced, one with 11 IET (Initiation, Elongation, Termination) and 1 AAT (Aminoacyl-tRNA Transferases) and the

other with 11 IET and 23 AAT proteins. (Contreras-Llano et al., 2020) with copyright of Nature research. https://creativecommons.org/licenses/by/4.0/

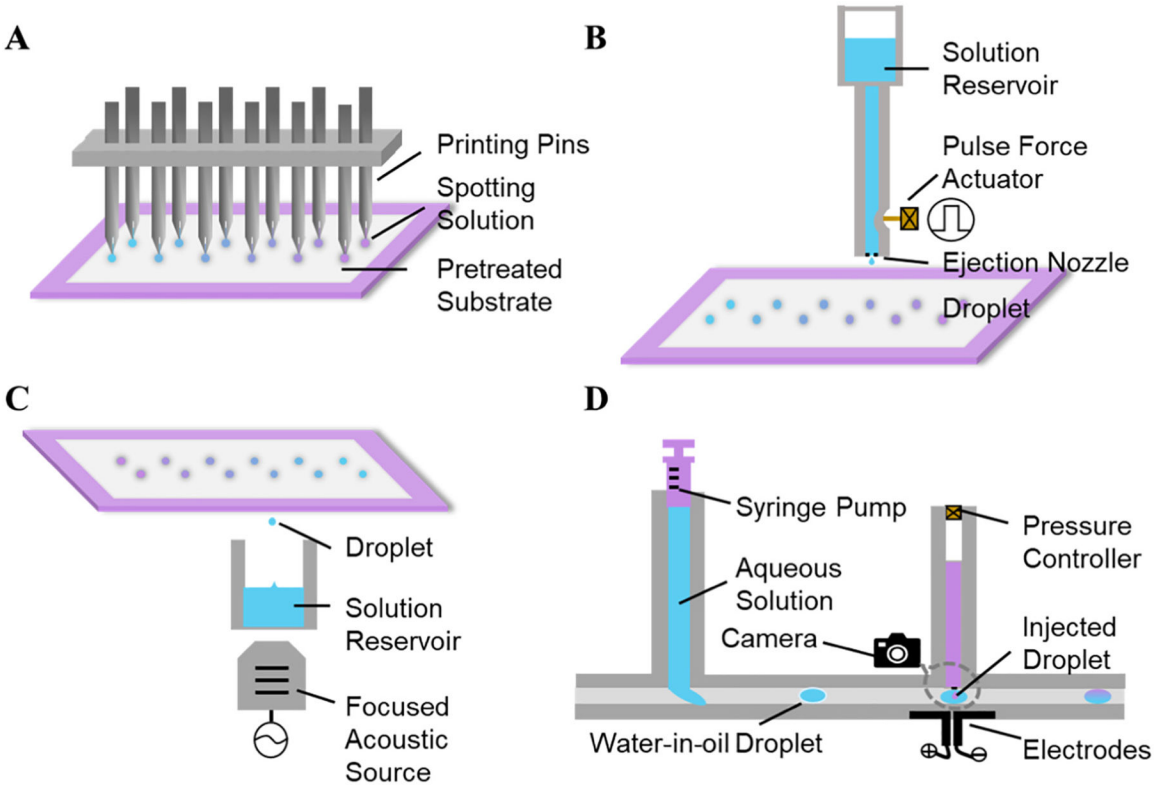

Fig. 4.

High-throughput and low-volume platforms for the assembly of protein networks. (A) Contact Pin-Printing: A manifold of pins transfers liquid by the contact between the pins and the receiving substrate. (Exemplar application: Swank et al., 2019) (B) Non-contact Inject Printing: A precisely controlled driving force generates droplets from a small ejection nozzle. The choice of driving forces includes electromagnetically actuated pins, piezoelectric actuators, and pneumatic drives. (Exemplar application: Fan et al., 2017) (C) Acoustic Inject Printing: A focused acoustic device transfers liquid from one container to a substrate without the uses of pipettes tips, pin tools, or ejection nozzle. (Exemplar application: Moore et al., 2018) (D) On-chip pico-injection: an electric field triggers the droplet fusion between a water-in-oil droplet and a controlled volume of reagent from a pressurized channel. (Exemplar application: Weiss et al., 2018).

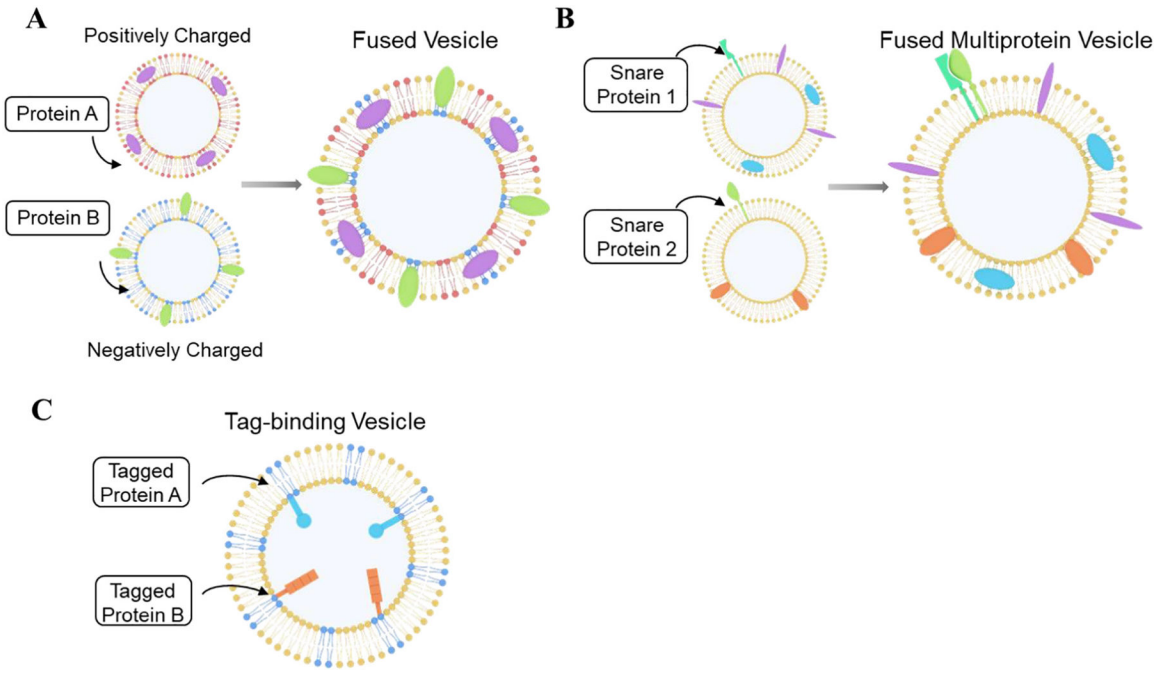

Fig. 5.

Schematic of three different strategies used to assemble protein networks. (A) Cartoon depicting the mechanism behind the charge-mediated fusion of a negatively charged vesicle and positively charged vesicle. (Exemplar application: Biner et al., 2016) (B) Cartoon illustration of SNARE-mediated reconstitution of multiple membrane proteins. (Exemplar application: Nordlund et al., 2014) (C) Cartoon illustration of the reconstitution of signaling pathways using membrane-bound protein kinase domain. (Exemplar application: Hui and Vale, 2014).